ผลของการเติมมีเทนต่อเซลล์อิเล็กโทรไลซิสชนิดออกไซด์แข็งสำหรับการผลิตก๊าซสังเคราะห์

นางสาวศิราภา ทองดี

วิทยานิพนธ์นี้เป็นส่วนหนึ่งของการศึกษาตามหลักสูตรปริญญาวิศวกรรมศาสตรมหาบัณฑิต
สาขาวิชาวิศวกรรมเคมี ภาควิชาวิศวกรรมเคมี
คณะวิศวกรรมศาสตร์ จุฬาลงกรณ์มหาวิทยาลัย
ปีการศึกษา 2557

EFFECT OF ADDING METHANE ON SOLID OXIDE ELECTROLYSIS CELL FOR SYNGAS PRODUCTION

Miss Sirapa Thongdee

A Thesis Submitted in Partial Fulfillment of the Requirements
for the Degree of Master of Engineering Program in Chemical Engineering
Department of Chemical Engineering
Faculty of Engineering
Chulalongkorn University
Academic Year 2014

Thesis Title	EFFECT OF ADDING METHANE ON SOLID OXIDE ELECTROLYSIS CELL FOR SYNGAS PRODUCTION
By	Miss Sirapa Thongdee
Field of Study	Chemical Engineering
Thesis Advisor	Assistant Professor Amornchai Arpornwichanop, D.Eng.

Accepted by the Faculty of Engineering, Chulalongkorn University in Partial Fulfillment of the Requirements for the Master's Degree

.....Dean of the Faculty of Engineering
(Professor Bundhit Eua-arporn, Ph.D.)

THESIS COMMITTEE

.....Chairman
(Associate Professor Soorathep Kheawhom, Ph.D.)
.....Thesis Advisor
(Assistant Professor Amornchai Arpornwichanop, D.Eng.)
.....Examiner
(Pimporn Ponpesh, Ph.D.)
.....External Examiner
(Assistant Professor Yaneeporn Patcharavorachot, D.Eng.)

ศิราภา ทองดี : ผลของการเติมมีเทนต่อเซลล์อิเล็กโทรไลซิสชนิดออกไซด์แข็งสำหรับการผลิตก๊าซสังเคราะห์ (EFFECT OF ADDING METHANE ON SOLID OXIDE ELECTROLYSIS CELL FOR SYNGAS PRODUCTION) อ .ที่ปรึกษาวิทยานิพนธ์หลัก: ผศ. ดร. อมรชัย อาภรณ์วิชานพ, 90 หน้า.

ไฮโดรเจนถูกพิจารณาเป็นระบบนำพาพลังงานสะอาด โดยในปัจจุบันการผลิตไฮโดรเจนจากเซลล์อิเล็กโทรไลซิสชนิดออกไซด์แข็งเป็นที่ได้รับความสนใจเนื่องจากสารตั้งต้นที่ใช้คือไอน้ำเท่านั้น นอกจากการผลิตไฮโดรเจนแล้ว การผลิตก๊าซสังเคราะห์จากเซลล์อิเล็กโทรไลซิสชนิดออกไซด์แข็งเป็นอีกหนึ่งทางเลือกในการลดก๊าซคาร์บอนไดออกไซด์เช่นกัน ซึ่งไอน้ำและก๊าซคาร์บอนไดออกไซด์ถูกเปลี่ยนเป็นไฮโดรเจนและคาร์บอนมอนออกไซด์ (ก๊าซสังเคราะห์) อย่างไรก็ตามการผลิตไฮโดรเจนและก๊าซสังเคราะห์จากเซลล์อิเล็กโทรไลซิสชนิดออกไซด์แข็งมีค่าใช้จ่ายในการดำเนินการที่สูงเนื่องจากมีการใช้พลังงานไฟฟ้าที่สูง สำหรับงานวิจัยนี้จะศึกษาเซลล์อิเล็กโทรไลซิสที่มีเชื้อเพลิงช่วยชนิดออกไซด์แข็ง ซึ่งในการดำเนินการนั้น ก๊าซมีเทนถูกป้อนเข้ามาที่ด้านแอโนดของเซลล์และเกิดปฏิกิริยารีฟอร์มมิงเพื่อผลิตไฮโดรเจน จากนั้นไฮโดรเจนที่ผลิตได้จะถูกใช้เพื่อผลิตกระแสไฟฟ้าสำหรับใช้ในกระบวนการอิเล็กโทรไลซิส จึงทำให้พลังงานที่ต้องการของเซลล์อิเล็กโทรไลซิสชนิดออกไซด์แข็งลดน้อยลง แบบจำลองไฟฟ้าเคมีถูกใช้เพื่อวิเคราะห์สมรรถนะของเซลล์อิเล็กโทรไลเซอร์ที่มีและไม่มีการป้อนมีเทน นอกจากนั้นผลของพารามิเตอร์ต่างๆ ได้แก่ ความหนาแน่นกระแสไฟฟ้า อัตราส่วนระหว่างไอน้ำและคาร์บอน อุณหภูมิ ความดัน และการใช้เชื้อเพลิงในเซลล์ ต่อสมรรถนะของเซลล์อิเล็กโทรไลเซอร์ยังถูกพิจารณาด้วย ผลจากการจำลองพบว่าสมรรถนะของเซลล์อิเล็กโทรไลซิสที่มีเชื้อเพลิงช่วยชนิดออกไซด์แข็งสูงกว่าเซลล์อิเล็กโทรไลซิสชนิดออกไซด์แข็งธรรมดาเนื่องจากใช้พลังงานไฟฟ้าน้อยกว่า นอกจากนั้นเซลล์อิเล็กโทรไลซิสที่มีเชื้อเพลิงช่วยชนิดออกไซด์แข็งสามารถดำเนินการได้โดยไม่จำเป็นต้องมีพลังงานไฟฟ้าจากข้างนอกเข้ามา

ภาควิชา วิศวกรรมเคมี ลายมือชื่อนิสิต .....

สาขาวิชา วิศวกรรมเคมี ลายมือชื่อ อ.ที่ปรึกษาหลัก .....

ปีการศึกษา 2557

5570398121 : MAJOR CHEMICAL ENGINEERING
KEYWORDS: HYDROGEN PRODUCTION / SYNGAS PRODUCTION / METHANE / MODELLING / PERFORMANCE ANALYSIS / SOLID OXIDE ELECTROLYSIS CELL

SIRAPA THONGDEE: EFFECT OF ADDING METHANE ON SOLID OXIDE ELECTROLYSIS CELL FOR SYNGAS PRODUCTION. ADVISOR: ASST. PROF. AMORNCHAI ARPORNWICHANOP, D.Eng., 90 pp.

Hydrogen is considered a clean energy carrier. At present, the production of hydrogen via a solid oxide electrolysis cell (SOEC) is of interest because steam is only used as a reactant. In addition, synthesis gas (syngas) production via the SOEC is a choice for decreasing carbon dioxide as steam and carbon dioxide are decomposed into hydrogen and carbon monoxide (syngas). However, the hydrogen and syngas production of SOEC have high operation cost due to high electrical energy consumption. In this work, a solid oxide fuel-assisted electrolysis cell (SOFEC) is studied. In the SOFEC operation, methane is added to the anode side of the SOEC and reformed to produce hydrogen. Hydrogen produced is used to produce electricity for use in the electrolysis process and thus, the energy demand of the SOEC can be reduced. An electrochemical model of the SOFEC is used to analyze the performance of the electrolyzer with/without the addition of methane. In addition, the effects of key operating parameters, such as current density, steam-to-carbon ratio, temperature, pressure and fuel utilization, on the electrolyzer cell perfor mance is discussed. The simulation results show that the performance of the SOFEC is higher than the conventional SOEC as it requires a lower power input. Furthermore, it is possible to run the SOFEC without an external electrical energy input.

Department: Chemical Engineering Student's Signature .....
Field of Study: Chemical Engineering Advisor's Signature .....
Academic Year: 2014

ACKNOWLEDGEMENTS

First of all, I would like to express my gratitude to my thesis advisor, Assistant Professor Amornchai Arpornwichanop, for his support, suggestion and guidance over the years.

Next, special thanks go to the thesis committee, Associate Professor Soorathep Kheawhom, Dr. Pimporn Ponpesh and Assistant Professor Yaneeporn Patcharavorachot, for their time and useful comments on my research.

Financial support by the Ratchadaphiseksomphot Endowment Fund of Chulalongkorn University, the Thailand Research Fund and the Computional Process Engineering Research Unit is gratefully acknowledged.

Last, I would also like to thank my family and my lovely friends in Control and Systems Engineering Research Center for all their support and help.

CONTENTS

Page

Page

LIST OF TABLES

Page

LIST OF FIGURES

Page

LIST OF FIGURES

Page

LIST OF FIGURES

Page

LIST OF FIGURES

Page

NOMENCLATURES

B_g	Permeability (m^2)
D_{AB}	Molecular binary diffusion coefficient of species A (m^2/s)
D^{eff}	Effective diffusion coefficient at cathode and anode (m^2/s)
$D^{eff}_{H_2O}$	Effective diffusion coefficient of steam (m^2/s)
D_{Ak}	Knudsen diffusion,
E	Open-circuit voltage (V)
E_{SOEC}	Open-circuit voltage of SOEC (V)
E_{SOFC}	Open-circuit voltage of SOFC (V)
E^0	Standard potential (V)
E^0_{SOEC}	Standard potential of SOEC (V)
E^0_{SOFC}	Standard potential of SOFC (V)
E_i	Activation energy at cathode and anode (J/mol K)
F	Faraday's constant
J	Current density (A/m^2)
$J_{0,a}$	Exchange current density at anode and cathode (A/m^2)
k_i	Pre-exponential factor ($\Omega^{-1}m^{-2}$)
$K_{eq,SR}$	Equilibrium constants of steam reforming reactions
$K_{eq,WGS}$	Equilibrium constants of water-gas shift reactions
LHV_{CO}	Low heating value of CO (J/mol)
LHV_{fuel}	Low heating value of fuel (J/mol)
LHV_{H2}	Low heating value of hydrogen (J/mol)
M_A	Molecular weight of substance
$\dot{N}_{CO,out}$	Outlet molar flow rate of CO (mol/s)
$\dot{N}_{fuel,in}$	Inlet molar flow rate of fuel (mol/s)
$\dot{N}_{H_{2,out}}$	Outlet molar flow rate of hydrogen (mol/s)
P	Operating pressure of SOEC (atm)
p_{H_2}	Partial pressure of hydrogen (N/m^2)

NOMENCLATURES

p_{H_2O}	Partial pressure of steam (N/m^2)
p_{O_2}	Partial pressure of oxygen (N/m^2)
r	Average electrode pore radius (m)
R	Gas constant (8.314 J/mol K)
T	Operating temperature (K)
V_{SOEC}	Cell voltage of SOEC (V)
V_{SOFC}	Cell voltage of SOFC (V)
V_{SOFEC}	Cell voltage of SOFEC (V)
U_{fuel}	Fuel utilization
U_{steam}	Steam utilization
W	Power (W)

Greek symbol

σ	Electric conductivity at cathode electrolyte and anode ($\Omega^{-1}m^{-1}$)
σ_{H_2}	Collision diameter of substance (m)
α	Charge transfer coefficient
e_{AB}	Lennard-Jones energy of molecular interaction
$\eta_{act,an}$	Anode activation overpotential (V)
$\eta_{act,cn}$	Cathode activation overpotential (V)
$\eta_{con,an}$	Anode concentration overpotential (V)
$\eta_{con,cn}$	Cathode concentration overpotential (V)
$\eta_{loss,SOEC}$	Overpotential losses of SOEC (V)
$\eta_{loss,SOFC}$	Overpotential losses of SOFC (V)
η_{ohmic}	Ohmic overpotential (V)
μ	Dynamic viscosity (kg/ m s)
ξ	Electrode tortuosity
ε	Electrode porosity

NOMENCLATURES

ε_{SOFEC}	Energy efficiency of SOFEC
Ω_D	Dimensionless diffusion collision integral
τ	Thickness (m)

Subscript

an	Anode
ca	Cathode
ele	Electrolyte
i	Component
SOEC	Solid oxide electrolysis cell
SOFC	Solid oxide fuel cell
SOFEC	Solid oxide fuel-assisted electrolysis cell

Super script

TPB	three phase boundary

CHAPTER I

INTRODUCRION

1.1 Importance and reasons

Nowadays, major energy source for everyday use comes from fossil fuels (oil, coal, and natural gas). The cause of the energy crisis can be traced fossil fuels reduction because of fossil fuels depletion. In addition, combustion of fossil fuels causes climate change due to increasing greenhouse gases. However, human still need to use energy for living, so they have found and improved alternative energies which should be similar to fossil fuels in the sense of quantity and efficiency in order to decrease fossil fuels usage for the future. Alternative energies, such as wind, solar, hydro, and hydrogen are considered a clean energy carrier and environmentally friendly. All of this, hydrogen is interesting because when combustion of hydrogen occurs, it does not release greenhouse gases. Furthermore, hydrogen has high heating value when it compares with other fuels combustion (Wanchanthuek, 2011). Hydrogen is used as a reactant in industries, such as hydrogenation process and it can use in fuel cell for producing electrical energy and thermal energy (Quakernaat, 1995). Moreover, hydrogen is also used to replace oil for transportation. At present, many automobile companies have improved their automobiles by using hydrogen as a fuel (De Groot, 2003).

Generally, there are a few of hydrogen in nature so it needs to be synthesized by conversion of raw materials. The processes of hydrogen production have various methods, for example, thermochemical, biochemical, photochemical, and

electrochemical process. Nowadays, hydrogen is mainly produced via thermochemical process from fossil fuels. In addition, photochemical process is low efficiency because of limitation of light intensity. Therefore, water/steam electrolysis via electrochemical process is interesting for hydrogen production because it uses only water as a reactant, which is decomposed into hydrogen and oxygen. In addition, the water/steam electrolysis is the cleanest method for producing hydrogen if it uses nuclear energy or renewable energy source for electricity. Electrolyzer for using in electrolysis process has many types such as an alkaline water electrolyzer, a proton exchange membrane electrolyzer, and a solid oxide electrolysis cell (SOEC). First and Second type of electrolyzer are lower temperature operation than the SOEC, which is operated under high temperature (700-1000 ˚C), thus the SOEC is lower electrical energy consumption and higher the reaction kinetics than other types of electrolyzer. Furthermore, there is heat generation as a by-product in the SOEC because of overpotential losses (activation overpotential, concentration overpotential, and ohmic loss). It can be used as heat source for steam fed into the SOEC (Ni et al., 2007). Although the SOEC is not used commercially to produce hydrogen owing to high cost for hydrogen production installation and large storage requirements (Laguna-Bercero, 2012), improvement and development of the SOEC is still necessary and interesting.

Despite the SOEC is attractive for hydrogen production, but it is expensive for commercial uses due to still high electrical energy consumption that is about 80% of total hydrogen production cost (Donitz et al., 1990). The energy consumption in the SOEC involves 2 parts: thermal energy and electrical energy. When temperature increases, the amounts of thermal energy consumption also increase, and the amounts of electrical energy consumption decrease. Because the operating costs almost come

from electrical energy consumption, thus the operating cost of the SOEC operated at high temperature is lower than other electrolyzers operated at low temperature. However, it is impossible to raise the temperature to high because of limitation of materials and catalysts of the SOEC, so many researchers search method to reduce the operating costs. Pham et al. (2000) were the first idea that can reduce electrical energy by adding a natural gas such as methane to react with oxygen at the anode side of the SOEC. The experiment showed a voltage reduction of as much as 1 V when compared to conventional steam electrolyzer (Martinez-Frias et al., 2003). After that, many researchers have focused on improving materials of a solid oxide fuel-assisted electrolysis cell (SOFEC). The cathode and anode side of the SOFEC work like the cathode side of the SOEC and the anode side of a SOFC, respectively. Tao et al. (2006) developed cathode materials for operated in the hybrid electrochemical devices (SOFC/SOEC/SOFEC) which can run reversible mode for co-production of hydrogen and electricity. Wang et al. (2007) also developed electrodes materials which are a Co-CeO_2-YSZ cathode and a Pd-C-CeO_2-YSZ anode in order to replaced Ni/YSZ electrodes for protecting the formation of carbon deposition from methane at high operating temperature. Luo et al. (2014) studied the performance of the SOFEC with anode gases of carbon monoxide and methane by experiment and elementary reaction modeling.

In addition to the usage of hydrogen as an alternative energy for decreasing carbon dioxide emission, the carbon dioxide can be reduced several ways, for example, carbon dioxide storage, and carbon dioxide recycling. In addition, the carbon dioxide is used as solvent, refrigerant, photosynthesis for plant growth, and a reactant. For instance, carbon dioxide reacts with methane for hydrogen and carbon

monoxide production called synthesis gas (syngas), which can continue to produce high-values chemical (Fouih & Bouallou, 2013). For example, syngas can convert into electrical energy by a fuel cell, and use as reactants in alcohol or hydrocarbon production from Fisher-Tropsch reactions. Furthermore, the SOEC can decompose carbon dioxide into carbon monoxide by same principle of hydrogen production of the SOEC so this method is a choice to decrease the carbon dioxide (Jensen et al., 2007). Moreover, the syngas can be produced in the SOEC simultaneously. At present, there are many studies which are interested in improvement of syngas production from the SOEC. However, the SOEC for syngas production is still high electricity cost. Therefore, the SOFEC is applied for producing syngas in order to reduce electrical energy consumption.

Thus, the aim of this study is to perform a model-based analysis of the SOFEC for hydrogen and syngas production by based on an electrochemical model. In addition, the SOFEC is compared with the conventional SOEC operation in terms of cell voltage, overpotentials, power density, and efficiency. Furthermore, the effect of key operating parameters, such as current density, steam-to-carbon ratio, temperature, pressure, and utilization on the SOFEC performance is analyzed.

1.2 Objective

To study effect of methane addition into the solid oxide fuel-assisted electrolysis cell (SOFEC) for improving performance in syngas production

1.3 Scopes

1. To develop the SOFEC model for hydrogen and syngas production by using electrochemical model, mass balance, and energy balance.
2. To study results of operating conditions for hydrogen and syngas production from the SOFEC.
3. To analysis performance and possibility of the SOFEC for syngas production

1.4 Thesis Overview

Chapter II reviews the literature about SOEC development for hydrogen, carbon monoxide, and synthetic gas (syngas) production, and mathematical model for simulation of the SOEC.

Chapter III presents the basic theory such as operation of the SOEC and SOFEC, and a mathematical model of the SOEC and the SOFEC.

Chapter IV shows model validation of the SOEC and the SOFEC for hydrogen production, the performance of the SOFEC for hydrogen production, and comparison between the SOEC and the SOFEC. Effect of configurations, inlet composition, operating pressure, operating temperature, and utilization are investigated.

Chapter V presents model validation of the SOEC for syngas production and the performance analysis of the SOFEC for syngas production. The SOEC for syngas production is compared with the SOFEC. The effect of configurations, inlet composition, pressure, temperature, and utilization are analyzed in terms of cell voltage, overpotential losses, power density, and efficiency.

Chapter VI gives the conclusion and suggestions of this dissertation

CHAPTER II
LISTERATURE REVIEWS

There are two main parts in the production of hydrogen and syngas by a solid oxide electrolysis cell (SOEC). The first part is development of the SOEC for hydrogen, carbon monoxide, and synthetic gas (syngas). In the second part, it is about mathematical model for simulation of SOEC.

2.1 SOEC development

Research on hydrogen production by SOEC began to be interesting when Donitz and Erdle (1985) experimented under HOT ELLY project . The project produces hydrogen by using the tubular SOEC at high temperature (1000 ºC) for long-term operation (1000 hours). After that, SOEC studies have steadily increased. The SOEC structure has two basic designs: tubular, and planar. From the experiment of Hino et al. (2004), the 12-cell tubular SOEC and can produce hydrogen at the maximum density of 44 $N \cdot cm^3/cm^2 \cdot h$ at 950 ºC and the maximum density of 38 $N \cdot cm^3/cm^2 \cdot h$ at 850 ºC, respectively. The results imply that the planar SOEC under operating at 850 ºC almost the same performance of the tubular SOEC obtained at 950 ºC. The tubular design facilitates sealing and lower cost of fabrication, on the other hand the planar design yields higher power densities and easier ease of fabrication. In the present, many researchers focus on the planar SOEC (Minh & Takahashi, 1995; Smolinka et al., 2015). In addition, there are three SOEC configurations: a cathode-supported, an electrolyte-supported, and an anode-supported. Ni et al. (2006) investigated the J-V characteristics of three configurations in a zero-dimensional

model and it was found that the anode-supported SOEC show the best performance because of lower cell voltage than other configurations, whereas Pay-Yu et al. (2011) studied a three-dimensional model of SOEC. The results show that the cathode-supported SOEC has higher performance than anode-supported and electrolyte-supported.

From the HOT ELLY project (Donitz et al., 1990), the cost of hydrogen production via the SOEC is still high and 80% of the total hydrogen production cost come from electrical energy consumption. Pham et al. (2000) are the first group that adds natural gas to the anode of SOEC to reduce electricity consumption. In addition, Martinez-Frias et al. experiment on single SOEC cells at 700 ºC. From the experiment, Natural gas that reacted with oxygen at anode of the SOEC cause voltage reduces as much as 1 V when compared to conventional steam electrolyzers. Furthermore, Martinez-Frias et al. (2003) found that carbon deposition on anode material happen when the SOEC operate at high temperature so avoidance of carbon deposition can be achieved by feeding steam with natural gas at the anode. Afterward, various studies of the solid oxide fuel-assisted electrolysis cell (SOFEC) have relied on experiments to synthesis and improve cell materials. Tao and Virkar (2006) developed cathode materials for operated in the hybrid electrochemical device which comprises a solid oxide fuel cell (SOFC) and the SOFEC for co-production of hydrogen and electricity directly from distributed natural gas or alternative fuels. Furthermore, Wang et al. (2007) used a Co-CeO_2-YSZ cathode and a Pd-C-CeO_2-YSZ anode replaced Ni-YSZ electrodes in order to protect the formation of carbon deposition from methane at high operating temperature. Moreover, Luo et al. (2014) studied the performance of SOFEC with anode gases of carbon monoxide and

methane by experiment and elementary reaction modeling. It is found that CH_4-SOFEC is higher performance than CO-SOFEC. The mechanism shows methane is not directly electrochemically oxidation but transferred by steam reforming to carbon monoxide and hydrogen for further electrochemical oxidation. Thus, SOFEC can produce not only hydrogen at the cathode but also generate electricity at the anode.

In addition to the above method, which can reduce electrical energy consumption, Udagawa et al. (2008) studied temperature control of the stack SOEC by the variation of the air flow rate at the anode of the SOEC. Besides temperature control, a voltage can decrease about 0.03 V from the SOEC which has only oxygen at the anode by endothermic operation but a small increase of electrical energy consumption occur when it operate in exothermic system. Furthermore, increasing of the air flow rate at the anode of SOEC provides enhanced cooling and heating during the exothermic and endothermic stack operation respectively, so the SOEC can be controlled temperature by adjusting air flow rate. Moreover for uniform temperature profile, there are advantages of a sweep air addition at the anode. First, the anode materials are safe because high chemical reactivity occurs when the anode has only of pure oxygen at high temperatures operation. Second, the mitigation of chromium deposition on the anode decreases the SOEC degradation rate (Becker et al., 2012). However, there are disadvantages of a sweep air. For example, pure oxygen from the SOEC is a valuable by-product to sell. Thus, if the right anode materials are used, the pure oxygen will be safe at high temperature operation (O'Brien et al., 2009). O'Brien et al. (2009) simulated a syngas production via the SOEC and the results are found that overall process efficiencies for cases with no sweep air at the anode were 1.0–1.5 percentage points higher than the sweep air cases. Moreover, temperature control by

sweep gas, the approach of integrating high temperature heat pipes to the SOEC can control temperature and reduce temperature gradients in the SOEC. The heat pipes are tubes or other cavities filled with small amounts of heat transfer liquid. The temperature gradients depend on the number of cell layers between the two heat pipe layers (Dillig & Karl, 2012).

Development of the SOEC for the future is to produce hydrogen without carbon in the process (carbon-free). The carbon is produced during electricity generation by using fossil fuels as energy source. Thus, renewable energy and nuclear energy are replaced as energy source for producing electricity. Elangovan et al. (2004) designed the high-temperature steam electrolysis (HTSE) system which coupled with the high-temperature gas-cooled reactor (HTGR). The HTGR is a high-temperature nuclear reactor which can generate the high-temperature heat and electrical power. The helium coolant is heated to outlet temperatures between 850 and 1000^{o}C. After that, the hot helium is divided into two parts. First, the hot helium serves as the working fluid in a gas-turbine power cycle. Second, the hot helium flows into a high-temperature heat exchanger for providing heat to the cathode inlet stream before fed into the HTSE. In addition, Mingyi et al. (2008) analyzed the overall efficiency of the HTSE and the HTGR coupled with the HTSE system by thermodynamic model. From the results, the efficiency of the HTGR coupled with the HTSE system is over two times higher than the conventional alkaline water electrolysis.

Many researchers not only develop hydrogen production by using clean energy but also popularly reduce carbon dioxide emission, which is the main cause of global warming, by using the SOEC for producing syngas. The advantages of a single SOEC for syngas production are lower cell resistance and reduction of the chance of

the carbon monoxide reduction reaction occurrence which causes carbon deposition on electrode surface. Matsuzaki and Yasuda (2000) studied the electrochemical oxidation of hydrogen and carbon monoxide at the interface of a porous electrode and an electrolyte. From the experiment, the electrochemical oxidation rate of hydrogen was about 2-3 times higher than that of carbon monoxide at 1073-1273 K because of the larger diffusion resistance of carbon monoxide than hydrogen on the electrode surface. In addition, the water-gas shift reaction was found to be much faster than the electrode reaction. Furthermore, the area specific resistance value of steam/carbon dioxide is similar to steam and it is lower than the area specific resistance value of carbon dioxide obviously. After that, there are many studies focus on using syngas from the SOEC as a reactant to produce other products. Fouih et al. (2013) studied the technical feasibility of ethanol production from syngas by using the SOEC. There are two main steps in the process of ethanol production. First, the syngas production is produced from co-electrolysis of carbon dioxide and steam by using the SOEC. Second, the ethanol production is produced from syngas in a catalytic reaction. According to the results, the total primary energy consumption of their study is more than the energy consumption of the usual ethanol production processes. In addition, Becker et al. (2012) simulated a thermochemical model of the SOEC for syngas production and subsequent conversion to liquid fuels such as gasoline and diesel via Fischer-Tropsch process. Moreover electrochemical reaction, reverse water gas shift reaction and methanation reaction are occurred in the SOEC. It is determined that operating the SOEC at low pressure (1.6 bar) versus higher pressure (5 bar) results in an efficiency gain of 2.6% and the methane is formed at high operating pressure. Besides high operating pressure, Li et al. (2013) studied co-electrolysis performance

and mechanisms in the SOEC at intermediate operating temperature (550-750^{o}C). From the experiment, methane is only detected in the gas products from the reactant composition of 28.6%H_2O + 14.3%CO_2 + 57.1%Ar, when the operating voltage of the electrolysis cell is higher than 2 V. There are two reaction pathways for methane production: reaction of carbon monoxide with hydrogen from electrochemical reaction (methanation reaction) and reactions of carbon element on the electrode surface with hydrogen (hydrogenation reaction).

2.2 SOEC modeling

The performance of the SOEC is improved not only by experiments but also by the simulation. Most simulation study of the SOEC is based on electrochemical model. The simulation of the SOEC in this review is divided into three parts: hydrogen production, carbon monoxide production, and syngas production.

First, electrochemical model of the SOEC for hydrogen production is used to study basic performance of the SOEC. There are two popular models: model from Ni et al. (2007b) and model from Udagawa et al. (2007) . Ni et al. (2007b) developed a theoretical model of the SOEC for hydrogen production by using an electrochemical model. The Butler-Volmer equation, Fick's model, and ohm's law were applied to the activation, concentration, and ohmic overpotential respectively which are the voltage loss. The model results were in good agreement with experimental data in term of cell voltage and current density. Udagawa et al. (2007) developed the electrochemical model and one-dimensional model. The model consists of the electrochemical model for the zero-dimensional model and the electrochemical model, a mass balance, and four energy balances for the one-dimensional model. Different from Ni et al.

(2007b)'s model, Udagawa et al. (2007)'s model was not validated with experimental data and some parameters were difference from Ni et al. (2007b)'s model. The model is neglected an anode concentration overpotential when oxygen only occurs at the anode. In addition, full voltage loss equations, the area specific resistance (ASR) based on experimental data is used to simplifier to calculate the cell voltage (Petipas et al., 2013) . From the aforementioned SOEC in the literature reviews part, the SOEC type is an oxygen ion-conducting SOEC (O-SOEC) which transport oxygen ions through the electrolyte to the anode, Furthermore O-SOEC, a proton-conducting SOEC (H-SOEC) which transport protons from the anode-electrolyte interface through the electrolyte to the cathode is attractive to produce hydrogen too. The advantages of the H-SOEC are needless hydrogen separation unit, hydrogen compression without a compressor, and the more potential of intermediate temperature operation. Ni et al. (2008) developed electrochemical model of the H-SOEC for hydrogen production. The simulation results agree well with experimental data. The model is different from the O-SOEC model at concentration overpotential and some parameters which depend on materials of the H-SOEC. Moreover, Demin et al. (2007) simulated the high temperature electrolyzer based on solid oxide co-ionic electrolyte. Both oxygen ions and protons can move across the electrolyte to another electrode simultaneously. Steam is fed into both the cathode and anode channel to occur proton conducting and oxygen conducting at the electrolyte respectively. As the results, the co-ionic SOEC is higher efficiency than the oxygen ion-conducting SOEC.

Second, carbon dioxide is used in electrolysis of the SOEC for carbon monoxide production. Ni (2010) developed two models of the SOEC for carbon

monoxide production: one-dimensional model and two-dimensional thermal-fluid model (consisting of the one-dimensional model and a computational fluid dynamics (CFD) model). The latter model considered heat and mass transfer in both gas channels and the porous electrodes. In addition, Zhang et al. (2013) developed an electrochemical model in zero dimension of the SOEC for carbon dioxide reduction. From the results, the anode-supported SOEC is the most preferable one in term of electrochemical performance.

Finally, the SOEC can produce syngas from steam/carbon dioxide mixture. O'Brien et al. (2009) developed the model to evaluate the performance of a large-scale high-temperature co-electrolysis plant which consists of pumps, compressors, heat exchanges, turbines, and the electrolyzer. The model of the electrolyzer part is simplified by using the zero dimensional model with using the ASR which is represented overpotential losses and depend on temperature only. In addition, the co-electrolysis process, coupled to a nuclear reactor, provides a means of recycling carbon dioxide back into a useful liquid fuel. Ni (2012a) developed a two-dimensional thermal model to study the heat/mass transfer and chemical/electrochemical reactions in the SOEC. The model is based on the CFD model, the electrochemical model, and the chemical model of the reversible water-gas shift and methanation reaction. As the results, It is found that the reversible water-gas shift is significant for the SOEC and methanation reaction is not favored at inlet temperature of 873-1073 K . Furthermore, Ni (2012b) developed the electrochemical model considering the reversible water gas shift at the cathode. The model is one-dimensional model along depth in the electrode for comparing the carbon monoxide fluxes at the cathode surface and the cathode-electrolyte interface. It is found that carbon monoxide is consumed or produced

depending on the rate of reversible water gas shift reaction in the porous cathode. Moreover, the rate of reversible water gas shift can be positive or negative, depending on the temperature and gas composition. Kazempoor and Braun (2014) developed the reversible electrochemistry, reactant chemistry, and the thermos-fluidic phenomena of the SOEC for syngas production. The model is one-dimensional model along cell length and the carbon dioxide electrochemical reaction can be neglected when the concentration of the steam supplied to the cell is high enough to support the water-gas shift reaction.

CHAPTER III

THEORY

A planar solid oxide cell structure consists of 4 parts: the interconnect, the cathode channel, the anode channel, and the solid structure (porous cathode, electrolyte, and porous anode). The electrochemical reactions take place at the electrodes (the cathode and the anode) and ions move through the electrolyte.

3.1 SOEC operation

3.1.1 SOEC operation for hydrogen production

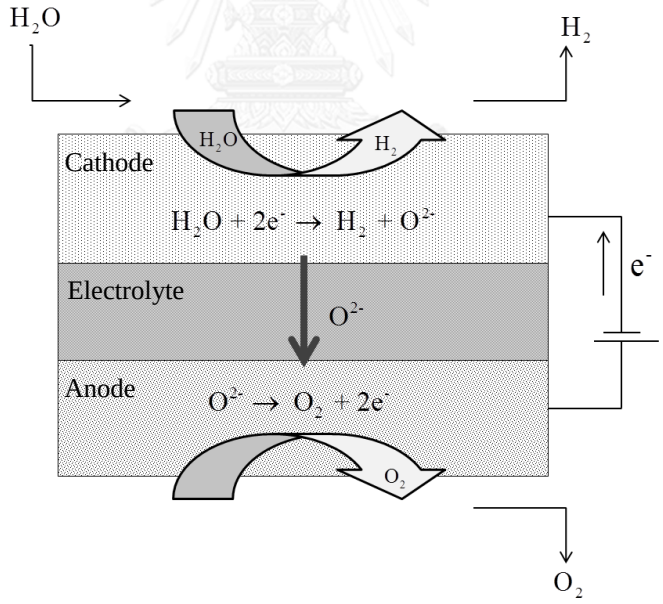

Figure 3.1 Schematic diagram of the SOEC for hydrogen production

Steam is fed into the cathode channel and diffuses to the porous cathode. Then, steam is decomposed by electrical energy to form hydrogen and oxygen ions (Equation (1)) at the triple-phase boundary (TPB). After that, oxygen ions are

transported through the electrolyte to the porous anode and oxidized to form oxygen gas (Equation (2)). The overall reaction of the SOEC for hydrogen production is shown in Equation (3).

At the cathode: $H_2O + 2e^- \rightarrow H_2 + O^{2-}$ (1)

At the anode: $O^{2-} \rightarrow \frac{1}{2}O_2 + 2e^-$ (2)

Overall: $H_2O \rightarrow H_2 + \frac{1}{2}O_2$ (3)

The most common materials used in the cathode is Ni/YSZ (Nickel/Yttria Stabilized Zirconium) and in the anode is LSM (Lanthanide, Strontium, and Manganese oxide)/YSZ and in the electrolyte is YSZ. In addition, the electrochemical reaction is occurred at the three phase boundary (TPB) where three phases (ions, electrons, gas phase) are contacted. In this case, three phases are oxygen ion, electron, and steam/hydrogen. For this work, the TPB takes place at the cathode-electrolyte interface and the anode-electrolyte interface.

3.1.2 SOEC operation for syngas production

Steam and carbon dioxide are fed into the cathode channel and diffuse to the porous cathode. After that, steam and carbon dioxide are decomposed by electrical energy to form hydrogen, carbon monoxide, and oxygen ions at the TPB. Hydrogen and carbon monoxide (syngas) diffuse through the cathode to the cathode channel, while oxygen ions are transported through the electrolyte to the anode and oxidized to form oxygen gas.

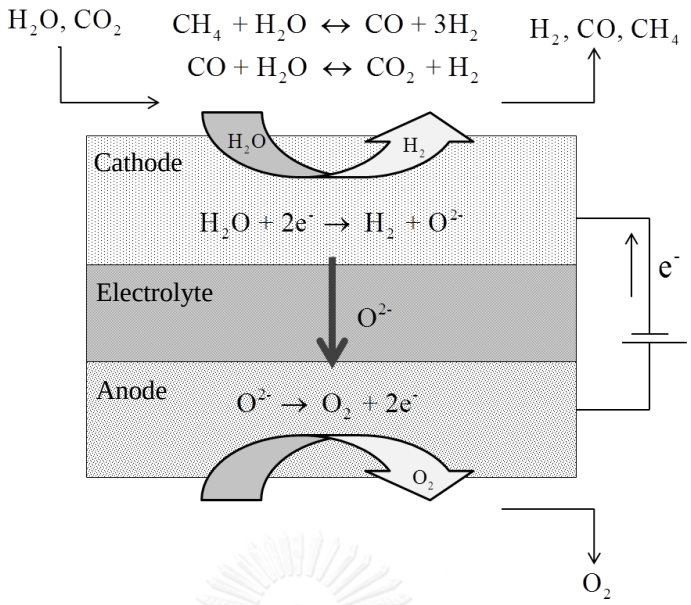

Figure 3.2 Schematic diagram of the SOEC for syngas production

In addition, not only electrochemical reactions but also other reactions are occurred at the cathode of the SOEC for syngas production which depended on inlet gas composition, operating condition, and cathode material. The reversible water-gas shift reaction (Equation (4)) is main reaction of carbon monoxide production in the SOEC. The reversible steam reforming (Equation (5)) is occurred to produce methane when the SOEC is operated at temperature below 973 K and nickel is used as catalyst. Therefore from the reversible water-gas shift reaction, the electrochemical reaction of carbon dioxide can be neglected when the concentration of the steam is high enough to support the water-gas shift reaction.(Kazempoor & Braun, 2014) so only the electrochemical reaction of hydrogen is occurred in the SOEC (Equation (6)) (Kazempoor & Braun, 2014; Matsuzaki & Yasuda, 2000),

At the cathode: $CO_2 + H_2 \leftrightarrow CO + H_2O$ (4)

$CO + 3H_2 \leftrightarrow CH_4 + H_2O$ (5)

$H_2O + 2e^- \rightarrow H_2 + O^{2-}$ (6)

At the anode: $O^{2-} \rightarrow \frac{1}{2}O_2 + 2e^-$ (7)

In addition, if the SOEC is operated at high cell voltage or low steam to carbon ratio (S/C), carbon deposition (Equation (8)) is happened at the electrode surface so catalyst performance is decreased (Redissi & Bouallou, 2013).

$CO \rightarrow C + \frac{1}{2}O_2$ (8)

To avoid carbon deposition and methane generation, the SOEC should be operated at proper cell voltage, S/C ratio, and operating temperature.

3.2 SOFEC operation

3.2.1 SOEC operation for hydrogen production

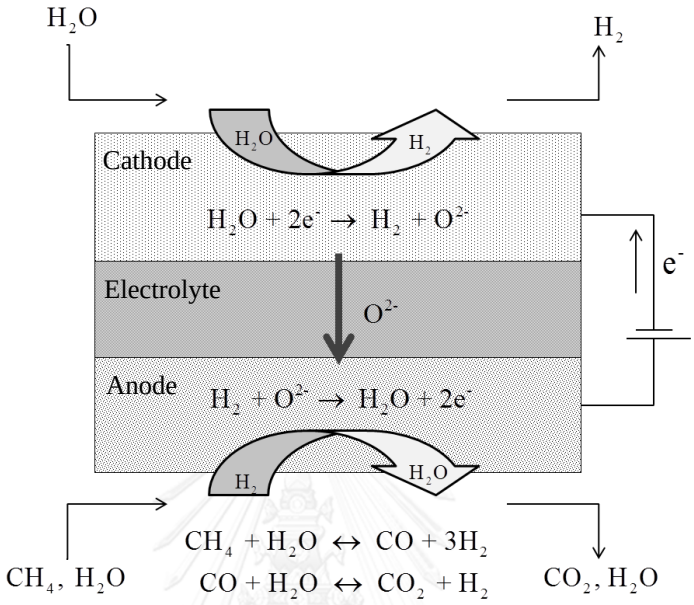

Figure 3.3 Schematic diagram of the SOFEC for hydrogen production

Steam is fed to the cathode channel and diffuses to the porous cathode. Steam is decomposed by electricity to form hydrogen and oxygen ions at the TPB. After that, oxygen ions are transported through the electrolyte to the porous anode. At the anode side, methane is fed into the anode channel. For avoid carbon deposition on the electrode surface that degrades electrode materials, high S/C ratio fed into the anode channel is needed (Novosel et al., 2008). Thus, two reactions are occurred in the SOFEC (the methane steam reforming followed by the water gas shift) (Equations (10)-(11)). Hydrogen production from the later reactions is diffused to the porous anode and it reacts with oxygen ion from the cathode to produce electricity (Equation (12)). Therefore, the SOFEC is operated same as the SOEC at the cathode side and the SOFC at the anode side.

At cathode side: $H_2O + 2e^- \rightarrow H_2 + O^{2-}$ (9)

At anode side: $CH_4 + H_2O \leftrightarrow CO + 3H_2$ (10)

$CO + H_2O \leftrightarrow CO_2 + H_2$ (11)

$H_2 + O^{2-} \rightarrow H_2O + 2e^-$ (12)

Overall: $CH_4 + 2H_2O \rightarrow CO_2 + 4H_2$ (13)

3.2.2. SOFEC operation for syngas production

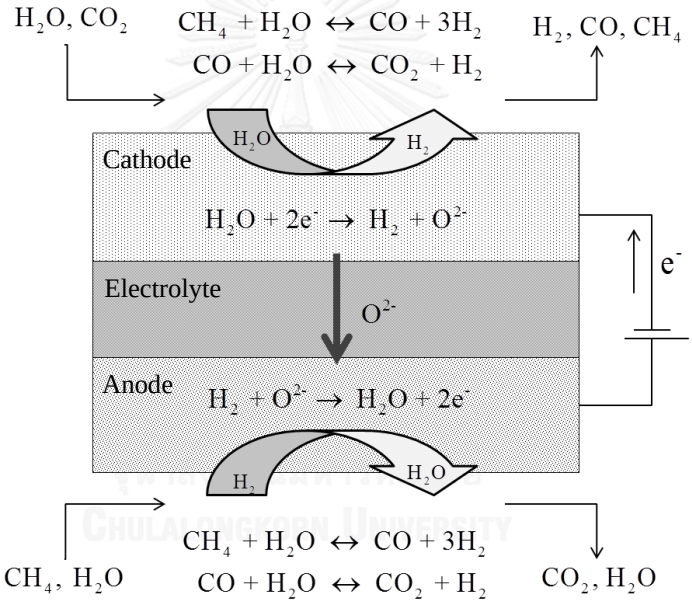

Figure 3.4 Schematic diagram of the SOFEC for syngas production

The operation at the cathode of the SOFEC is same as at the cathode of the SOEC for syngas production. In the same way, the operation at the anode of the SOFEC is same as at the anode of the SOFC.

At the cathode: $CO_2 + H_2 \leftrightarrow CO + H_2O$ (14)

$CO + 3H_2 \leftrightarrow CH_4 + H_2O$ (15)

$H_2O + 2e^- \rightarrow H_2 + O^{2-}$ (16)

At anode side: $CH_4 + H_2O \leftrightarrow CO + 3H_2$ (17)

$CO + H_2O \leftrightarrow CO_2 + H_2$ (18)

$H_2 + O^{2-} \rightarrow H_2O + 2e^-$ (19)

3.3 Thermodynamics of the SOEC

For hydrogen or carbon monoxide production, the SOEC at high operating temperature uses electrical energy lower than at low operating temperature. According to Figure 3.5, total energy demand (ΔH) is:

$$\Delta H = \Delta G + T\Delta S \quad (20)$$

where ΔG is electric energy demand (kJ/mole), TΔS is heat demand (kJ/mole).

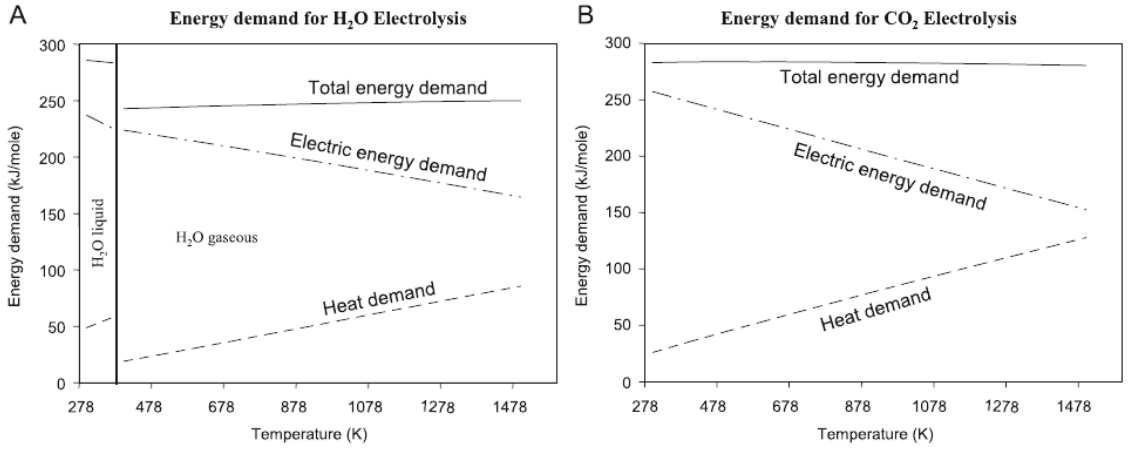

Figure 3.5 Energy consumption for hydrogen and carbon monoxide production

From Figure 3.5, energy demand depends on temperature; therefore, when operating temperature is increased, electric energy demand is decreased, while heat demand is increased. In addition, total energy demand for hydrogen or carbon monoxide production is not dependent on operating temperature because it changes little when operating temperature is varied. Thus, the advantages of high operating temperature of the SOEC are low electrical energy consumption, fast reaction kinetics, and low internal resistance.

3.4 The SOEC model

To simulate a SOEC, an electrochemical model is considered. The assumptions of the model are as follows: steady state operation, one-dimensional along gas flow direction, adiabatic process, no pressure drop, ideal gas behavior for all gases, and only hydrogen that can be electrochemically oxidized and reduced at the anode and cathode respectively.

3.4.1 Electrochemical model

3.4.1.1 Hydrogen production

The SOEC demand external electrical energy for decomposing steam into hydrogen and oxygen. Electrical energy (power density input) can be calculated from cell voltage and current density. The open-circuit voltage (OCV), which is an ideal voltage for the SOEC, is calculated from the Nernst equation (Equation (21)). The OCV for the SOEC means the minimum voltage required to produce hydrogen.

$$E = E^0 + \frac{RT}{2F}\ln\left[\frac{P_{H_2}P_{O_2}^{0.5}}{P_{H_2O}}\right] \quad (21)$$

where E is the open-circuit voltage (V), E^0 is the standard potential (V) which is involved with the Gibbs free energy change of reaction ($E^0 = \Delta G/2F$), R is the gas constant (J $mol^{-1}K^{-1}$), T is the operating temperature (K), F is the Faraday's constant (C mol^{-1}), P_{H_2}, P_{O_2}, and P_{H_2O} are the partial pressure (bar) of hydrogen, oxygen, and steam, respectively.

When the SOEC is operated, the cell voltage is higher than the OCV because of overpotential losses (Equation (22)). For this simulation, the cathode, electrolyte, and anode are made from Ni/YSZ, YSZ, and LSM/YSZ respectively.

$$V_{SOEC} = E + \eta_{conc} + \eta_{act} + \eta_{ohmic} \quad (22)$$

where V_{SOEC} is the cell voltage of the SOEC (V), η_{conc} is the concentration overpotentials (V), η_{act} is the activation overpotentials (V), and η_{ohmic} is the ohmic overpotentials (V).

From electrochemical model, hydrogen production rate of the electrochemical reaction can be evaluated from Equation (23). It is based on Faraday's law as:

$$R = \frac{J}{2F} \quad (23)$$

here, R is the rate of electrochemical reaction (mol s^{-1} m^{-2}), and J is a current density (A m^{-2})

The concentration overpotential is caused by the mass transport of components in porous electrode. Because of reactions in the electrodes, the concentration of reactants is reduced so gas diffusion resistance in electrode is occurred obviously. The

concentration or pressure of gases is changed between the TPB, the bulk flow, and the electrode surface. The concentration overpotential can be written as:

$$\eta_{conc,ca} = \frac{RT}{2F}\ln\left[\frac{P_{H_2,ca}^{TPB} P_{H_2O,ca}}{P_{H_2,ca} P_{H_2O,ca}^{TPB}}\right] \tag{24}$$

$$\eta_{conc,an} = \frac{RT}{2F}\ln\left[\left(\frac{P_{O_2,an}^{TPB}}{P_{O_2,an}}\right)^{0.5}\right] \tag{25}$$

here, the subscripts ca and an are the cathode and anode respectively, the superscript TPB is the three phase boundary where electrochemical reaction is occurred, and P_{O_2} is the partial pressure of oxygen (Pa). Pressure of hydrogen and steam at the TPB can be calculated from the one-dimensional diffusion equation for equimolar counter-current mass transfer (Equations (26)-(27)) (Chan et al., 2001).

$$P_{H_2,ca}^{TPB} = P_{H_2,ca} + \frac{RTJ\tau_{ca}}{D_{ca}^{eff} 2F} \tag{26}$$

$$P_{H_2O,ca}^{TPB} = P_{H_2O,ca} - \frac{RTJ\tau_{ca}}{D_{ca}^{eff} 2F} \tag{27}$$

where, τ is thickness of the electrodes (m), and D_{ca}^{eff} is an effective diffusivity of the cathode (m^2s^{-1}).

The effective diffusivity consists of both molecular diffusion, which is the molecule-molecule interaction, and Knudsen diffusion, which is the molecule-pore wall interaction. The effective diffusivity of the cathode which is average of gases effective diffusivity can be written as:

$$D_{ca}^{eff} = \left(\frac{P_{H_2O,ca}}{P}\right) D_{H_2}^{eff} + \left(\frac{P_{H_2,ca}}{P}\right) D_{H_2O}^{eff} \tag{28}$$

The effective diffusivity of the A component can be calculated as follows:

$$\frac{1}{D_A^{eff}} = \frac{\xi}{\varepsilon}\left(\frac{1}{D_{AB}} + \frac{1}{D_{Ak}}\right) \tag{29}$$

where, ξ is an electrode tortuosity, ε is an electrode porosity, D_{AB} is the molecular binary diffusion coefficient (m^2s^{-1}), and D_{Ak} is Knudsen diffusion coefficient of species A (m^2s^{-1}).

For straight and round pores, D_{Ak} can be expressed as:

$$D_{Ak} = 97r\sqrt{\frac{T}{M_A}} \tag{30}$$

here, r is the average pore radius (m), and M_A is the molecular mass of A.

The molecular binary diffusion coefficient can be calculated by using the Chapman-Enskog theory (Equation (31)).

$$D_{AB} = 0.0018583\left(\frac{1}{M_A} + \frac{1}{M_B}\right)^{0.5} \frac{T^{1.5}}{P\sigma_{AB}^2\Omega_{DAB}} \tag{31}$$

where, σ_{AB} is the collision diameter (Å), and Ω_D is the collision integral based on the Lennard-Jones potential which is the dimensionless parameter.

$$\sigma_{AB} = \frac{\sigma_A + \sigma_B}{2} \tag{32}$$

$$\Omega_D = \frac{1.06036}{\tau^{0.15610}} + \frac{0.193}{\exp(0.47635\tau)} + \frac{1.03587}{\exp(1.52996\tau)} + \frac{1.76474}{\exp(3.89411\tau)} \tag{33}$$

$$\tau = \frac{kT}{e_{AB}} \tag{34}$$

where, e_{AB} is the Lennard-Jones energy of molecular interaction.

Because only oxygen is occurred at the anode, pressure of oxygen at the TPB causes a pressure gradient in the anode so oxygen is transported in the electrode by permeation, instead of diffusion. The oxygen pressure at the TPB (Equation (35)) is solved from the oxygen flux by using Darcy's law (Meng Ni, Michael K. H. Leung, & Dennis Y. C. Leung, 2006).

$$P_{O_2,an}^{TPB} = \sqrt{P_{O_2,an}^2 + \left(\frac{JRT\mu\tau_{an}}{2FB_g}\right)} \tag{35}$$

where, μ is the dynamic viscosity of oxygen (kg m^{-1} s^{-1}) which is a function of temperature (Todd & Young, 2002), B_g is the flow permeability, which can be determined by the Kozeny–Carman relationship.

$$B_g = \frac{\varepsilon^3}{72\xi(1-\varepsilon)^2}(2r)^2 \tag{36}$$

The activation overpotential is voltage loss from kinetics of the reaction. In addition, the voltage loss, which is happened, causes to decrease the rate of electrochemical reaction. The electrochemical reaction is occurred when energy is higher than activation energy. Butler-Volmer equation (Equation (37)) is presented for the activation overpotential which relates with charge transfer of the reaction.

$$J = J_{0,i}\left[\exp\left(\frac{2(1-\alpha)F\eta_{act,i}}{RT}\right) - \exp\left(\frac{-2\alpha F\eta_{act,i}}{RT}\right)\right], \text{ i = ca, an} \tag{37}$$

where, subscript i is the cathode and the anode, $J_{0,i}$ is the exchange current density for the electrode (A m^{-2}), and α represents the transfer coefficient (usually taken to be 0.5).

The exchange current density which is kinetic parameter to determine the local electrode current density at open-circuit voltage can be expressed as:

$$J_{0i} = \frac{RT}{2F} k_i \exp\left[\frac{-E_i}{RT}\right], \text{ i = ca, an} \quad (38)$$

where, k_i is the pre-exponential factor ($\Omega^{-1}m^{-2}$), and E_i is the activation energy (J mol^{-1}).

The ohmic loss is caused by the resistance of ions and electrons conduction through the electrolyte and the electrode, respectively. It depends on configurations and cell conduction. Ohm's law used for calculation can be obtained:

$$\eta_{ohmic} = J\left(\frac{\tau_{ca}}{\sigma_{ca}} + \frac{\tau_{ele}}{\sigma_{ele}} + \frac{\tau_{an}}{\sigma_{an}}\right) \quad (39)$$

$$\sigma_{ele} = 33.4\times10^3 \exp\left(\frac{-10.3\times10^3}{T}\right) \quad (40)$$

where, τ_{ca}, τ_{ele}, τ_{an} are thickness of the cathode, electrolyte, and anode, respectively (m), and σ_{ca}, σ_{ele}, σ_{an} are electric conductivity of the cathode, ionic conductivity of the electrolyte, and electric conductivity of the anode, respectively ($\Omega^{-1}m^{-1}$).

3.4.1.2 Syngas production

The SOEC for syngas production uses electricity for decomposing steam and carbon dioxide into syngas and oxygen. Power density demand can be calculated from cell voltage and current density. The OCV and the voltage losses (the activation overpotential, the concentration overpotential, and the ohmic loss) of the SOEC for syngas production are calculated same as the SOEC for hydrogen production

(Equations (21)-(40)) because the electrochemical reaction of carbon dioxide is not considered in the SOEC for syngas production. In addition, most carbon dioxide is used in the reversible water-gas shift reaction.

For zero-dimensional model of the SOEC for syngas production, the equilibrium models of the methane steam reforming and the water-gas shift reaction are proper to use at the cathode channel. The equilibrium constant can be calculated as:

$$K_{eq,SR} = 1.0267 \times 10^{10} \exp\left(-0.2513Z^4 + 0.3665Z^3 + 0.5810Z^2 - 27.134Z + 3.2770\right) \quad (41)$$

$$K_{eq,WGS} = \exp\left(-0.2935Z^3 + 0.6351Z^2 + 4.1788Z + 0.3196\right) \quad (42)$$

$$Z = \frac{1000}{T} - 1 \quad (43)$$

where, $K_{eq,SR}$, $K_{eq,WGS}$ are the equilibrium constants of steam reforming and water-gas shift reactions from Haberman and Young (2004).

3.4.2 Electrochemical model of the SOFEC

3.4.2.1 Hydrogen production

The SOFEC demand external electrical energy for decomposing steam into hydrogen and oxygen that same as the SOEC. Electrical energy (power density input) can be calculated from cell voltage and current density. For the SOFC, the OCV means the maximum voltage that produce electricity. On the other hand, the OCV for the SOEC means the minimum voltage required to produce hydrogen. In addition, when the SOFC and the SOEC are operated, the cell voltage is lower and higher than the OCV for the SOFC and the SOEC, respectively, because of irreversible losses.

The electrochemical model of the solid oxide fuel cell (SOFC) and the SOEC are used to develop the electrochemical model for the SOFEC. For this simulation, the electrodes and electrolyte are made of Ni-YSZ and YSZ, respectively.

For the SOFEC, the cell voltage comes from the combination of SOFC and SOEC voltage. It only has oxygen ion in the electrolyte so concentration of oxygen is not occurred in the electrode. The cell voltage (V_{SOFEC}) can be derived as:

$$V_{SOFEC} = V_{SOEC} - V_{SOFC} \tag{44}$$

$$V_{SOFEC} = (E_{SOEC} + \eta_{loss,SOEC}) - (E_{SOFC} - \eta_{loss,SOFC}) \tag{45}$$

where, V_{SOEC} and V_{SOFC} are the cell voltage of the SOEC and the SOFC, respectively (V), E_{SOEC} and E_{SOFC} are the OCV of the SOEC and SOFC, respectively (V), $\eta_{loss,SOEC}$ and $\eta_{loss,SOFC}$ are the overpotential losses of the SOEC and SOFC, respectively (V).

Because of same the standard potential between the SOEC and SOFC, E^0_{SOEC} and E^0_{SOFC} from Equation (46) are neglected. Thus, Equation (47) is the cell voltage for the SOFEC.

$$V_{SOFEC} = \left(E^0_{SOEC} + \frac{RT}{2F} \ln\left[\frac{P_{H_2,ca} P^{0.5}_{O_2,an}}{P_{H_2O,ca}} \right] + \eta_{loss,SOEC} \right) - \left(E^0_{SOFC} + \frac{RT}{2F} \ln\left[\frac{P_{H_2,an} P^{0.5}_{O_2,ca}}{P_{H_2O,an}} \right] - \eta_{loss,SOFC} \right) \tag{46}$$

$$V_{SOFEC} = \frac{RT}{2F} \ln\left[\frac{P_{H_2,ca} P_{H_2O,an}}{P_{H_2O,ca} P_{H_2,an}} \right] + \eta_{conc} + \eta_{act} + \eta_{ohmic} \tag{47}$$

The concentration overpotential (η_{conc}) can be written as:

$$\eta_{conc,ca} = \frac{RT}{2F} \ln\left[\frac{P^{TPB}_{H_2,ca} P_{H_2O,ca}}{P_{H_2,ca} P^{TPB}_{H_2O,ca}} \right] \tag{48}$$

$$\eta_{conc,an} = \frac{RT}{2F} \ln \left[\frac{P_{H_2O,an}^{TPB} P_{H_2,an}}{P_{H_2O,an} P_{H_2,an}^{TPB}} \right] \quad (49)$$

It is assumed that these reactions take place at electrode-electrolyte interface. $P_{H_2,ca}^{TPB}$ and $P_{H_2O,ca}^{TPB}$ are calculated from Equation (26) and (27) respectively. Pressure of hydrogen and steam at the anode-electrolyte interface (at the TPB) can be calculated from the one-dimensional diffusion equation for equimolar counter-current mass transfer as follow (Chan et al., 2001):

$$P_{H_2,an}^{TPB} = P_{H_2,an} - \frac{RTJ\tau_{an}}{D_{an}^{eff} 2F} \quad (50)$$

$$P_{H_2O,an}^{TPB} = P_{H_2O,an} + \frac{RTJ\tau_{an}}{D_{an}^{eff} 2F} \quad (51)$$

here, D_{an}^{eff} is an effective diffusivity of the anode (m^2s^{-1}), which can be calculated from Equations (28)-(34) for the anode gases.

The activation overpotential and ohmic loss of the SOFEC can be calculated same as the SOEC (Equations (37)-(39)) but parameters for calculation are depended on materials of the electrodes. In addition, the equilibrium models of the methane steam reforming (Equation (41)) and the water-gas shift reaction (Equation (42)) are used at the anode channel for zero-dimensional model of the SOFEC.

3.4.2.2 Syngas production

The OCV and the voltage losses (the activation overpotential, the concentration overpotential, and the ohmic loss) of the SOEC for syngas production are calculated same as the SOEC for hydrogen production (Equations (21)-(40))

because the electrochemical reaction of carbon dioxide is not considered in the SOEC for syngas production. In addition, most carbon dioxide is used in the reversible water-gas shift reaction.

For zero-dimensional model of the SOFEC for syngas production, the equilibrium models of the methane steam reforming and the water-gas shift reaction are proper to use at the cathode channel. The equilibrium constant can be calculated from Equations (41) and (42).

3.4.3 SOFEC utilization

In order to calculate molar flow rate of composition, steam utilization at cathode and fuel utilization at anode of the SOFEC are specified.

$$U_{steam} = \frac{JLW}{2F\,\dot{N}_{H_2O,in}} \tag{52}$$

$$U_{fuel} = \frac{JLW}{2F\,\dot{N}_{CH_4,in}} \tag{53}$$

where, U_{steam} and U_{fuel} are steam utilization and fuel utilization, respectively, L and W are cell length and cell width (m), respectively, and $\dot{N}_{H_2O,in}$ and $\dot{N}_{CH_4,in}$ are the inlet flow rate of steam and methane (mol s^{-1}), respectively.

3.4.4 SOFEC performance

The performance of the SOFEC is presented in term of the power density (W) and energy efficiency as follows:

$$W = IV \tag{54}$$

$$\varepsilon_{SOFEC} = \frac{LHV_{H_2}\,\dot{N}_{H_2,out} + LHV_{CO}\,\dot{N}_{CO,out}}{IV + \sum LHV_{fuel}\,\dot{N}_{fuel,in}} \quad , \text{V} > 0 \qquad (55)$$

$$\varepsilon_{SOFEC} = \frac{LHV_{H_2}\,\dot{N}_{H_2,out} + LHV_{CO}\,\dot{N}_{CO,out} + IV}{\sum LHV_{fuel}\,\dot{N}_{fuel,in}} \quad , \text{V} < 0 \qquad (56)$$

where $LHV_{H_2}, LHV_{CO}, LHV_{fuel}$ are the lower heating value of hydrogen, carbon monoxide, and fuel respectively (J mol^{-1}), $\dot{N}_{H_2,out}, \dot{N}_{CO,out}, \dot{N}_{fuel,in}$ are the outlet flow rate of hydrogen, carbon monoxide, and the inlet flow rate of fuel (mol s^{-1}), I is a current (A).

CHAPTER IV

SOLID OXIDE FUEL ASSISTED ELECTROLYSIS CELL FOR HYDROGEN PRODUCTION

This chapter presents the performance analysis of the SOFEC for hydrogen production. At the cathode, steam is fed to the cathode of the SOFEC and it is decomposed into hydrogen and oxygen ion. After that, oxygen ion is transported through the electrolyte to the anode. At the anode, methane and steam are fed to the anode channel, so the steam reforming and the water-gas shift reaction are occurred. Next, hydrogen from the steam reforming and the water-gas shift reaction diffuses to the porous anode and reacts with oxygen ion from the electrolyte in order to generate electricity. The simulation uses the model from section 3.4.2.1 as electrochemical model and the performance is analyzed in terms of voltage, power density, and efficiency. First of all, the SOFEC is compared with the SOEC for hydrogen production. Next, the configurations of the SOFEC are investigated in order to determine which configurations are proper to use. After that, the key operating parameters such as inlet compositions, operating pressure, operating temperature and utilization are considered.

4.1 Model input parameters and operating conditions

For the SOFEC, Table 4.1 and Table 4.2 show the model input parameters and operating conditions, respectively. Generally, SOEC materials are Ni-YSZ at the cathode, YSZ at the electrolyte, and LSM-YSZ at the anode. But anode material is changed for the SOFEC because the anode material is replaced with Ni-YSZ which is

commonly used for methane oxidation in the anode side. In addition, the methane oxidation is caused carbon deposition on Ni-YSZ material. In order to prevent carbon deposition on the anode, steam should be added in steam-to-carbon ratio (S/C) more than 2 (Alzate-Restrepo & Hill, 2008).

Table 4.1 Model input parameters of the SOFEC for hydrogen production

Parameters	Value
Cathode pre-exponential factor, k_{ca}	$654\times10^{9}\ \Omega^{-1}m^{-2}$
Cathode activation energy, E_{ca}	$140\times10^{3}\ J\cdot mol^{-1}$
Cathode electric conductivity, σ_{ca}	$80\times10^{3}\ \Omega^{-1}m^{-1}$
For the SOEC	
Anode pre-exponential factor, k_{an}	$235\times10^{9}\ \Omega^{-1}m^{-2}$
Anode activation energy, E_{an}	$137\times10^{3}\ J\cdot mol^{-1}$
Anode electric conductivity, σ_{an}	$8.4\times10^{3}\ \Omega^{-1}m^{-1}$
For the SOFEC	
Anode pre-exponential factor, k_{an}	$654\times10^{9}\ \Omega^{-1}m^{-2}$
Anode activation energy, E_{an}	$140\times10^{3}\ J\cdot mol^{-1}$
Anode electric conductivity, σ_{an}	$80\times10^{3}\ \Omega^{-1}m^{-1}$
Electrode porosity, ε	0.3
Electrode tortuosity, ξ	6
Average pore radius, r	0.5 μm
Cell length, L	0.4 m
Cell width, W	0.1 m

Parameters (continue)	Value
Cathode thickness, τ_{ca}	500 μm
Electrolyte thickness, τ_{ele}	10 μm
Anode thickness, τ_{an}	50 μm
For comparison of support structures	
For cathode-supported cell	
Cathode thickness, τ_{ca}	500 μm
Electrolyte thickness, τ_{ele}	50 μm
Anode thickness, τ_{an}	50 μm
For electrolyte-supported cell	
Cathode thickness, τ_{ca}	50 μm
Electrolyte thickness, τ_{ele}	500 μm
Anode thickness, τ_{an}	50 μm
For anode-supported cell	
Cathode thickness, τ_{ca}	50 μm
Electrolyte thickness, τ_{ele}	50 μm
Anode thickness, τ_{an}	500 μm

Table 4.2 Operating conditions of the SOFEC for hydrogen production

Parameters	Value
Operating temperature, T	1073 K
Operating pressure, P	1 bar
Average current density, J	7000 A/m^2
Steam utilization at cathode	0.8
Fuel utilization at anode	0.8
Cathode stream inlet composition	10 mol% H_2, 90 mol% H_2O
For the SOEC	
Anode stream inlet composition	100 mol% O_2
For the SOFEC	
Anode stream inlet composition	S/C = 2

4.2 Model validation

4.2.1 The SOEC for hydrogen production

The model of the SOEC for hydrogen production (Section 3.4.1.1) is validated with experiments from Momma et al. (2005). The cathode inlet composition is 60% H_2O and 40% H_2. The thickness of Ni-YSZ cathode, YSZ electrolyte, LSM–YSZ anode are 100, 1000, 100 μm, respectively. The results at different operating temperature (Figure 4.1) show that the simulation result is good agreement with the experimental data. When the SOEC operate at high current density, the SOEC can produce more hydrogen, so it use high electricity consumption. This model can be used to study the performance of the SOEC for hydrogen production.

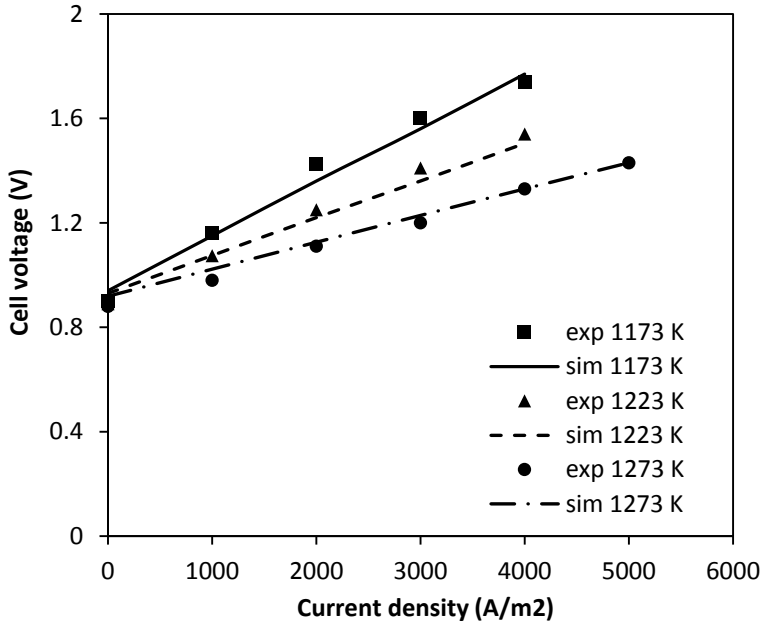

Figure 4.1 Comparison of polarization curves between experimental and model results of the SOEC for hydrogen production

4.2.2 The SOFEC for hydrogen production

The SOFEC model results were compared with experimental data. Wang et al. (2008) experimented the SOFEC for producing hydrogen at operating temperature of 973 K. The cathode stream inlet composition consisted of H_2O/H_2 = 13 and P_{H2O} = 0.57 atm. The YSZ thickness of 50 μm sandwiched between 15 and 300 μm thick porous YSZ layers. In addition, pre-exponential factor = 854×10^9 $\Omega^{-1}m^{-2}$ is used to manipulate the model parameter. The comparison of the experimental and model results in term of polarization curves at different anode stream inlet composition (CH_4:H_2O:CO_2 = 10:40:80 and CH_4:H_2O:CO_2 = 10:20:10) is shown in Figure 4.2. As a result, the model results have demonstrated good agreement with the experimental data. However, the OCV of model is less than experiment because the low reactivity of methane and equilibrium not being established for high methane concentrations on the anode materials. According to the SOFEC operation, there is negative net cell

voltage in Figure 4.2 at low current density. It means that the SOFEC can produce both electricity and hydrogen. In addition, the SOFEC can produce only hydrogen at positive net cell voltage. Moreover, the SOFEC can operate without external electricity input at zero net cell voltage.

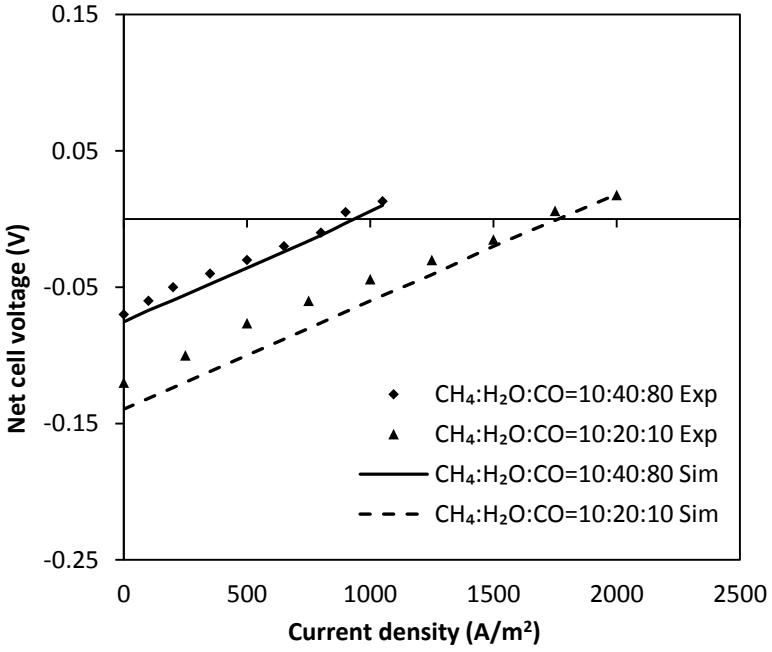

Figure 4.2 Comparison of polarization curves between experimental and model results of the SOFEC for hydrogen production

4.3 Results and discussion

4.3.1 Comparisons between the SOEC and the SOFEC for hydrogen production

The SOEC and the SOFEC are same operation at the cathode of cell but they are different at the anode. For the SOEC, the anode of cell has only oxygen gas. On the other hand, the inlet compositions of anode are methane and steam for the SOFEC. The comparison between the SOEC and the SOFEC for hydrogen production is based on electrochemical model. The simulation results are shown in Figure 4.3 and Figure 4.4. Figure 4.3 shows the performance of the SOEC versus the SOFEC in

terms of cell voltage and power density at different current density. As a result, the voltage of the SOFEC is about 1 V lower than the SOEC and it is occurred negative voltage at current density about 0-7000 A/m^2. Thus in this current density range, external power is unnecessary for hydrogen production and the SOFEC can produce both hydrogen and electricity at the same time. In addition, at zero voltage represents the SOFEC that can produce hydrogen by without using external electricity and generating electricity. Furthermore, the power consumptions are shown in Figure 4.3. As a result, the SOFEC is less power input than the SOEC obviously. Negative power input on the SOFEC represents both hydrogen and power are generated. The maximum power generation takes place at about 3000 A/m^2. At negative cell voltage, the SOFEC can reduce more than 100% of electrical energy demand compared with the SOEC. It means that the SOFEC not only operate without electrical energy but also can generate electricity. At positive cell voltage, the SOFEC can reduce more than 90% of electrical energy demand compared with the SOEC. From Figure 4.4, overpotential losses of the SOEC and the SOFEC are compared. Activation overpotential is major overpotential losses. Ohmic loss is the second largest overpotential losses, and the last is concentration overpotential. For the SOFEC operation, activation and concentration overpotential are different from the SOEC operation because of different materials and inlet composition at the anode side. Table 4.3 presents comparison of parameters between the SOEC and the SOFEC for hydrogen production at current density of 7000 A/m^2. Hydrogen production rate is based on current density only so the SOFEC has same flow rate with the SOEC. To sum up, the SOFEC has a better performance than the SOEC in terms of electrical energy consumption.

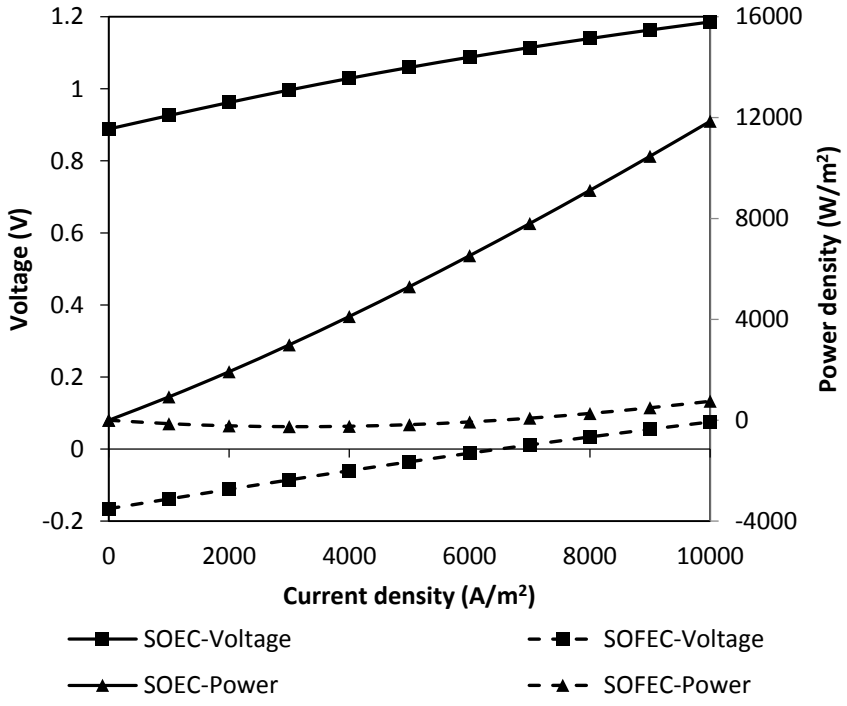

Figure 4.3 Comparison of cell voltage and power density between the SOEC and the SOFEC for hydrogen production

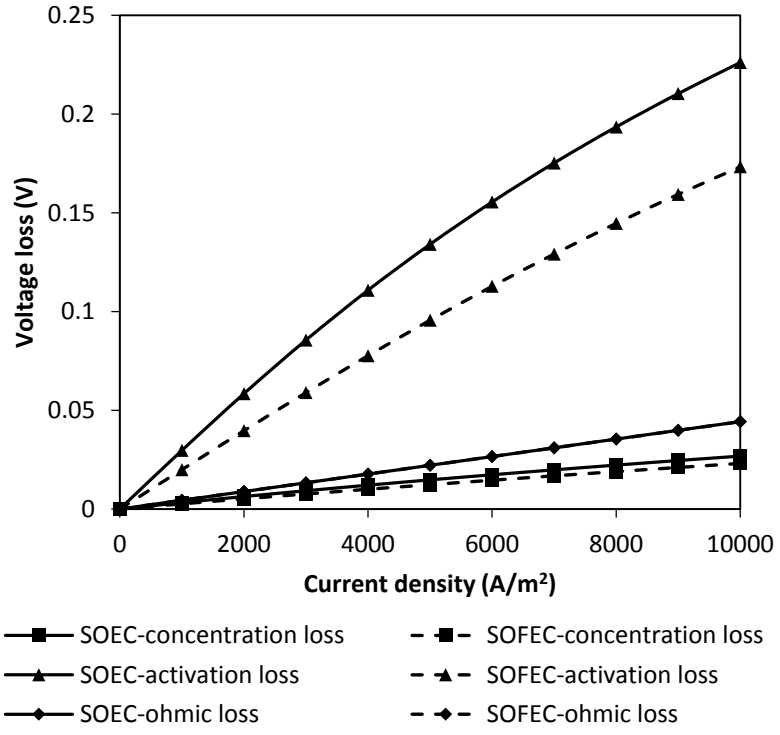

Figure 4.4 Comparison of overpotential losses between the SOEC and the SOFEC for hydrogen production

Table 4.3 Comparison of the SOEC and the SOFEC for hydrogen production at current density of 7000 A/m^2

	SOEC	SOFEC
Current density (A/m^2)	7000	7000
Net cell voltage (V)	1.11	0.01
Power density (W/m^2)	7801	81
Concentration overpotential (V)	0.0198	0.0168
Activation overpotential (V)	0.1752	0.1291
Ohmic loss (V)	0.031	0.031
Hydrogen production rate (mol/s)	0.00145	0.00145
Steam inlet flow rate at cathode (mol/s)	0.00181	0.00181
Methane inlet flow rate at anode (mol/s)	0	0.00045

Figure 4.5 presents flow rate of hydrogen production and steam inlet at the cathode of the SOEC and SOFEC, and fuel inlet at anode of the SOFEC at differnt current density. It is found that hydrogen production rate depends on current density only because hydrogen is produced from electrochemical reaction. Other gases depend on hydrogen production, utilization, mole fraction of inlet composition.

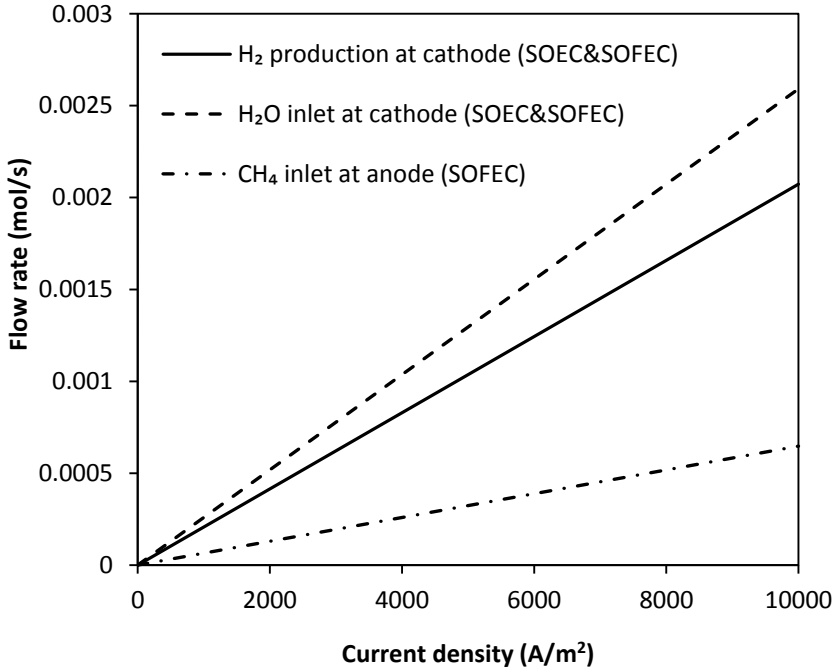

Figure 4.5 Flow rate of hydrogen production at the cathode, steam inlet at cathode, and fuel inlet at anode at differnt current density of SOEC and SOFEC

4.3.2 Effect of configurations

4.3.2.1 Effect of support structures

The SOFEC has three configurations: cathode-supported, electrolyte-supported, and anode-supported. To study performance of the SOFEC, the configurations are also significant. From Figure 4.6, three configurations were compared in terms of cell voltage and power density, respectively. It was found that the electrolyte-supported SOFEC is higher power consumption than the cathode-supported and anode-supported SOFEC definitely because it has the highest ohmic loss that is depended on electrolyte thickness in Figure 4.8. Thus, the electrode-supported cell is appropriate for producing hydrogen from the SOFEC. From Figure 4.7, concentration overpotential at the cathode and anode are compared at different supported cell. ‘nconc,ca’ and ‘nconc,an’ in Figure 4.7 represent concentration

overpotential at the cathode and anode, respectively. It was found that the anode side of the anode-supported SOFEC is higher concentration overpotential than the cathode side of the cathode-supported SOFEC although they have same thickness electrode, because mole fraction of steam and hydrogen in the electrode have an affect on concentration overpotential. Hydrogen from steam reforming and water gas shift reaction at the anode side of the anode-supported cell is harder diffuses to the TPB for electrochemical reaction than steam at the cathode side of the cathode-supported cell. In addition, the anode side of the anode-supported cell is lower effective diffusivity than the cathode side of the cathode-supported cell, so steam between at the TPB and at bulk are different obviously that cause high concentration overpotential. Thus, the anode-supported is higher power density than the cathode-supported slightly. As above-mentioned, the cathode-supported SOFEC is proper to use for hydrogen production.

Besides effect of support structure, the electrode and electrolyte thickness are considered for the performance of the SOFEC too. It is analyzed in next section.

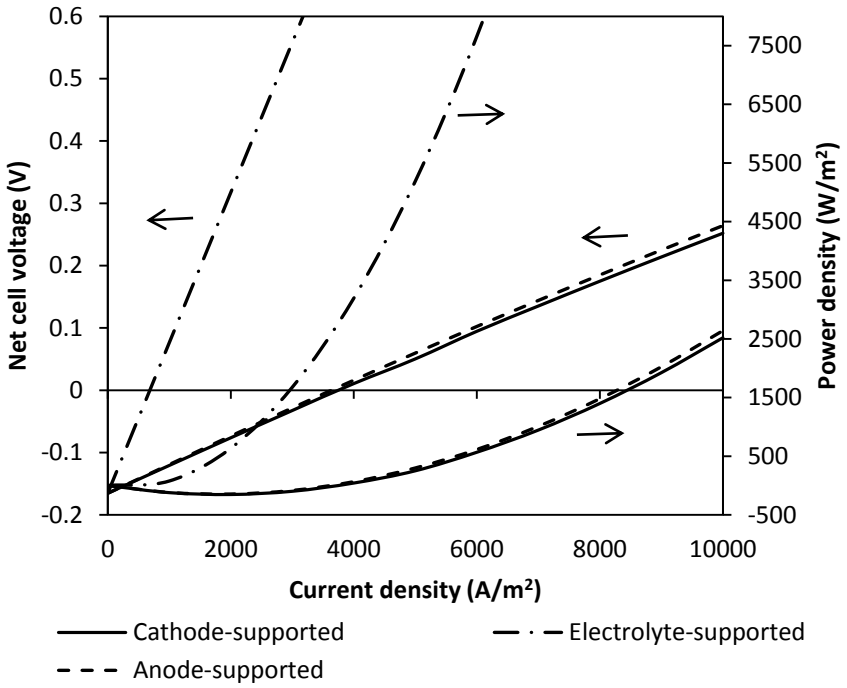

Figure 4.6 Comparison of net cell voltage and power density with different supported cell of the SOFEC for hydrogen production

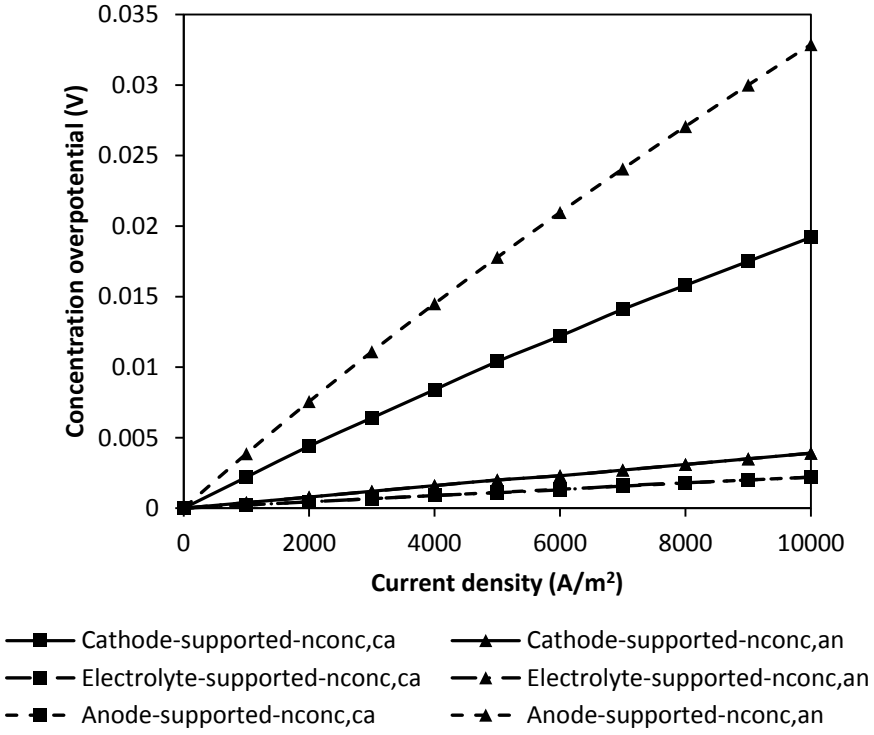

Figure 4.7 Comparison of concentration overpotential with different supported cell of the SOFEC for hydrogen production

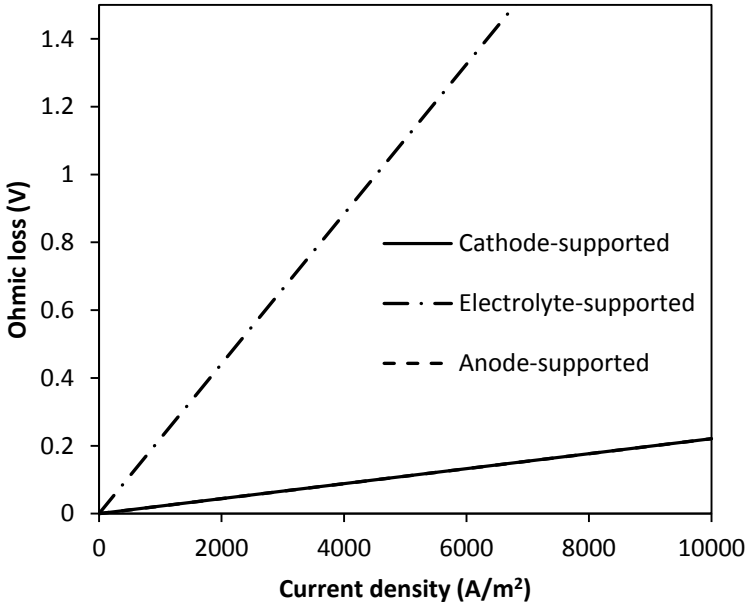

Figure 4.8 Comparison of ohmic loss with different supported cell of the SOFEC for hydrogen production

4.3.2.2 Effect of cathode thickness

The performance of the SOFEC is considered in terms of the cathode thickness. Because the cathode-supported SOFEC for hydrogen production is investigated for this simulation, the cathode thickness of 100 μm, 500 μm, and 1000 μm are compared (the electrolyte thickness of 10 μm and the anode thickness of 50 μm are fixed). From Figure 4.9, when the cathode thickness increases, the power density consumption increases so it causes low performance. Similarly, concentration overpotential also increases (Figure 4.10). Because the diffusion of gases from the cathode channel to the cathode-electrolyte interface is more difficult when increasing the cathode thickness thus concentration overpotential increase. In addition, when the cathode thickness significantly increases, the ohmic loss is unchanged. Thus, the ohmic loss does not depend on cathode thickness.

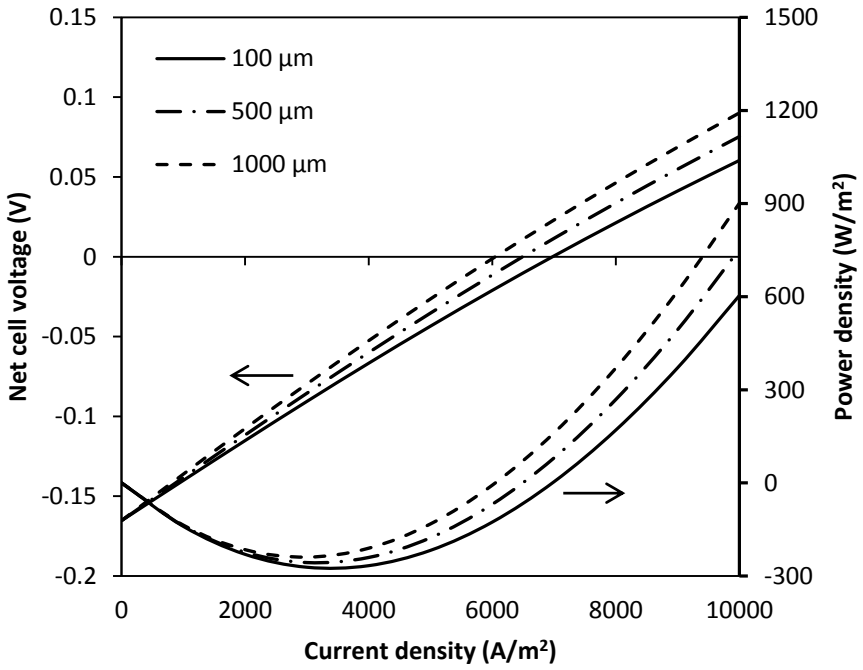

Figure 4.9 Effect of cathode thickness on cell voltage and power density of the SOFEC for hydrogen production

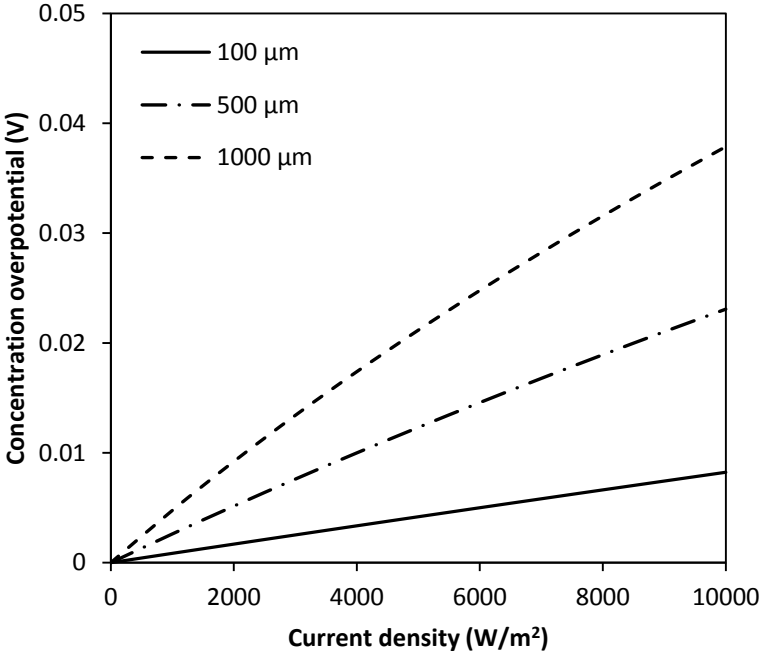

Figure 4.10 Effect of cathode thickness on concentration loss of the SOFEC for hydrogen production

4.3.2.3 Effect of electrolyte thickness

The effect of the electrolyte thickness is shown in Figure 4.11 and Figure 4.12. The electrolyte thickness of 10 μm, 30 μm, and 50 μm are considered (the cathode thickness of 500 μm and the anode thickness of 50 μm are fixed). It was found that the electrolyte thickness significantly has an affect on the performance of the SOFEC because power density increase when the electrolyte thickness slightly increase (Figure 4.11). Similarly, ohmic loss increases obviously with increasing electrolyte thickness (Figure 4.12) because it has more resistance in the electrolyte. Therefore, the low electrolyte thickness should be used for the SOFEC. In addition, the possibility of the thinnest electrolyte thickness which avoid cracking of the YSZ thin film is 10 μm (X. Wang et al., 2012; Yu et al., 2012; Zou et al., 2011).

4.3.2.4 Effect of anode thickness

The anode thickness of 25 μm, 50 μm, and 100 μm are simulated for the cathode-supported SOFEC (the cathode thickness of 500 μm and the electrolyte thickness of 10 μm are fixed). As a result, the cell voltage and power density slightly increase when the anode thickness increases (Figure 4.13). The concentration overpotential increase with increasing the anode thickness (Figure 4.14) but it slightly causes the cell voltage increase. In addition, ohmic loss is same as before increasing the anode thickness. Consequently, the anode thickness is hardly important on the performance of the SOFEC.

Therefore, the cathode thickness of 500 μm, the electrolyte thickness of 10 μm, and the anode thickness of 50 μm are considered in order to study the performance of the SOFEC in next section.

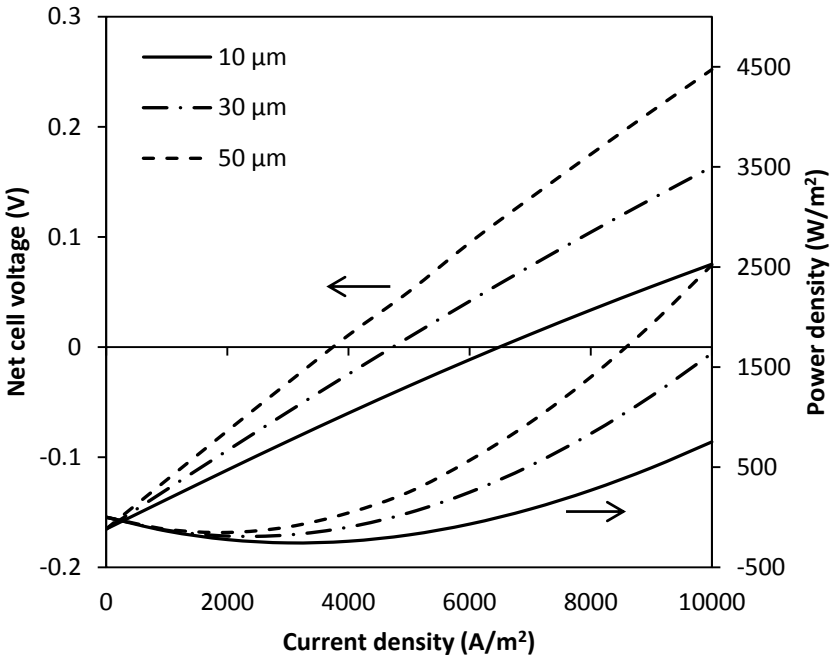

Figure 4.11 Effect of electrolyte thickness on cell voltage and power density of the SOFEC for hydrogen production

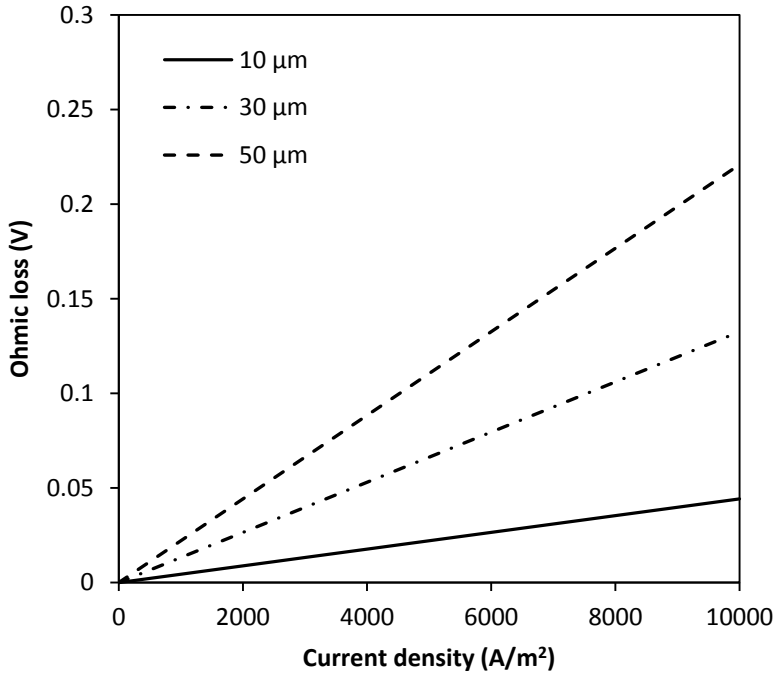

Figure 4.12 Effect of electrolyte thickness on ohmic loss of the SOFEC for hydrogen production

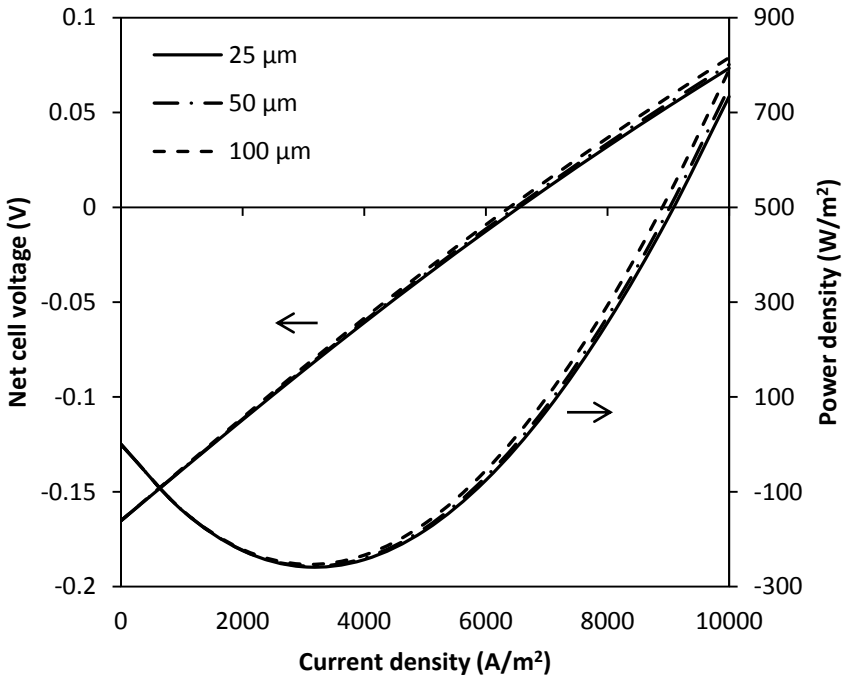

Figure 4.13 Effect of anode thickness on cell voltage and power density of the SOFEC for hydrogen production

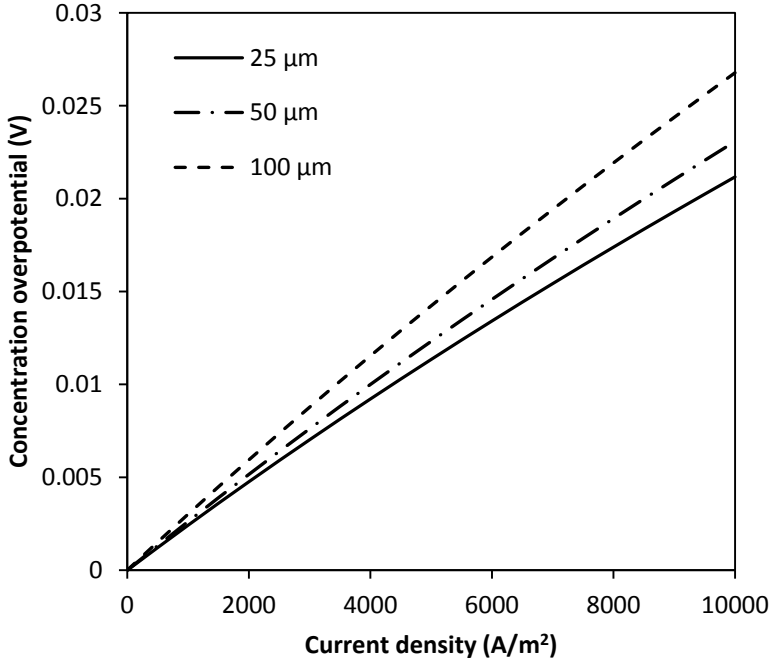

Figure 4.14 Effect of anode thickness on concentration loss of the SOFEC for hydrogen production

4.3.3 Effect of inlet composition

4.3.3.1 Effect of steam fraction

For the SOFEC operation, Steam is fed to the cathode to produce hydrogen. However, not only steam but also hydrogen is fed to the cathode too because hydrogen is a reducing gas which is used for avoiding oxidation of the Ni electrode (J. E. O'Brien et al., 2012). To investigate effect of inlet composition, steam molar fraction at the cathode was varied from 0.5 to 0.9 and steam to carbon ratio at the anode side was fixed at 2. It was found that power density consumption decreased and efficiency increased with increasing steam molar fraction (Figure 4.15). The power density decreases because the cell voltage decreases (Figure 4.16). In addition, the open-circuit voltage (OCV) decrease when steam molar fraction increase according to the Nernst equation (Equation (21)). From Figure 4.16, concentration overpotential slightly increased with increasing steam molar fraction because diffusion increased when steam molar fraction increased, steam at the TPB and at bulk are similar values but hydrogen at the TPB and at bulk are different values because of high hydrogen production, thus concentration increased.

4.3.3.2 Effect of steam to carbon ratio

At the anode of the SOFEC, steam is added to avoid carbon formation on the electrode materials. Thus the steam to carbon ratio has an affect on the performance of SOFEC. The steam to carbon ratio was varied from 2 to 6 and the steam molar fraction at the cathode was fixed at 0.9. From Figure 4.17, when steam to carbon ratio increased, the power density consumption increased because of low hydrogen at the SOFEC anode. In addition, the efficiency slightly decreased although the power

consumption obviously increased because the key of efficiency is the fuel molar flow rate. From Figure 4.18, when steam to carbon ratio increased, cell voltage increased because of increasing the OCV and the concentration overpotential less changed. Thus, steam to carbon ratio increases with electrical energy consumption increases.

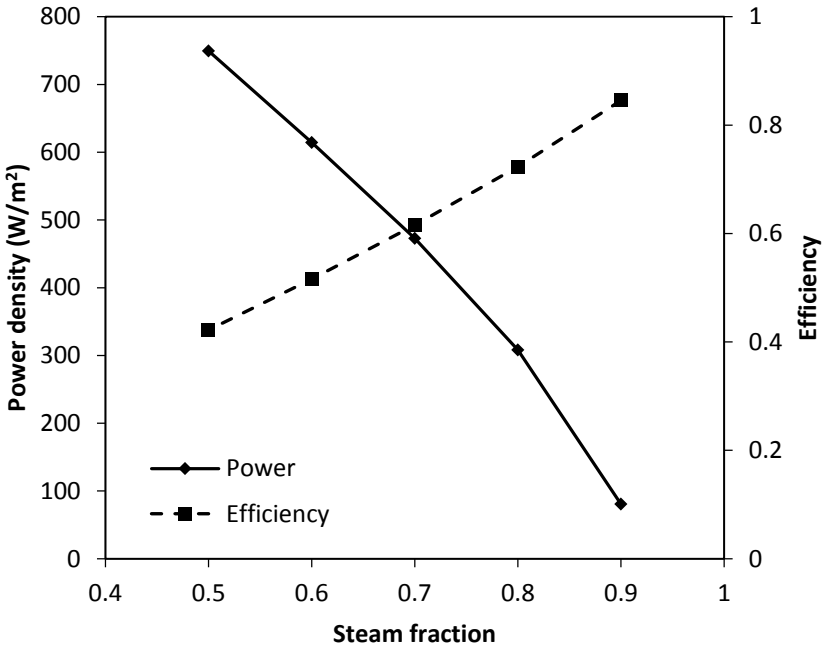

Figure 4.15 Effect of inlet steam fraction at the cathode of SOFEC in terms of power density and efficiency for hydrogen production

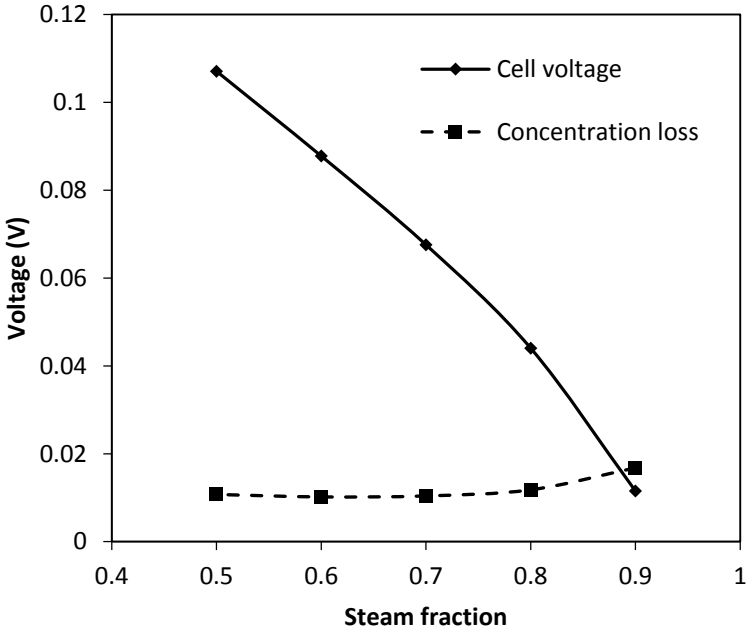

Figure 4.16 Effect of inlet steam fraction at the cathode of SOFEC in terms of cell voltage and concentration loss for hydrogen production

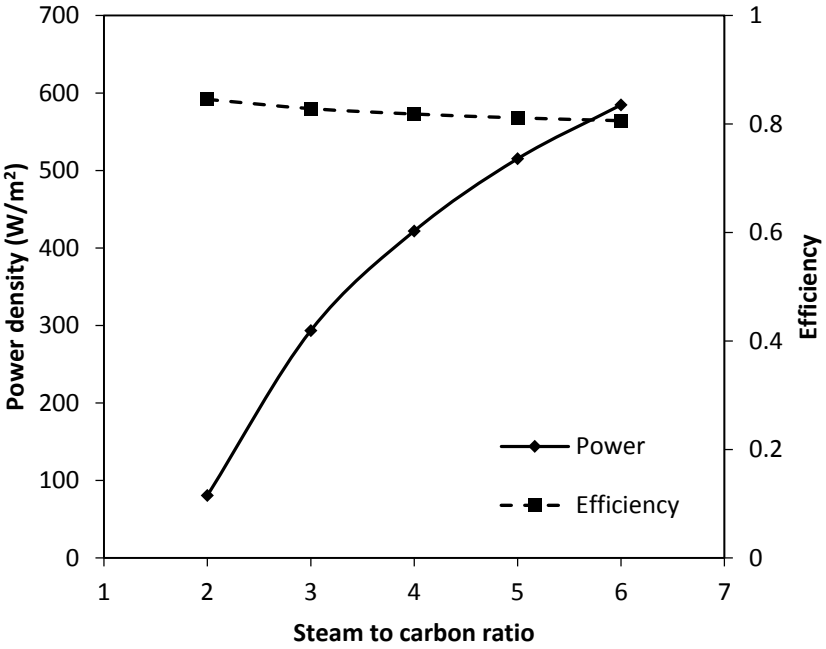

Figure 4.17 Effect of inlet steam to carbon ration at the anode of SOFEC in terms of power density and efficiency for hydrogen production

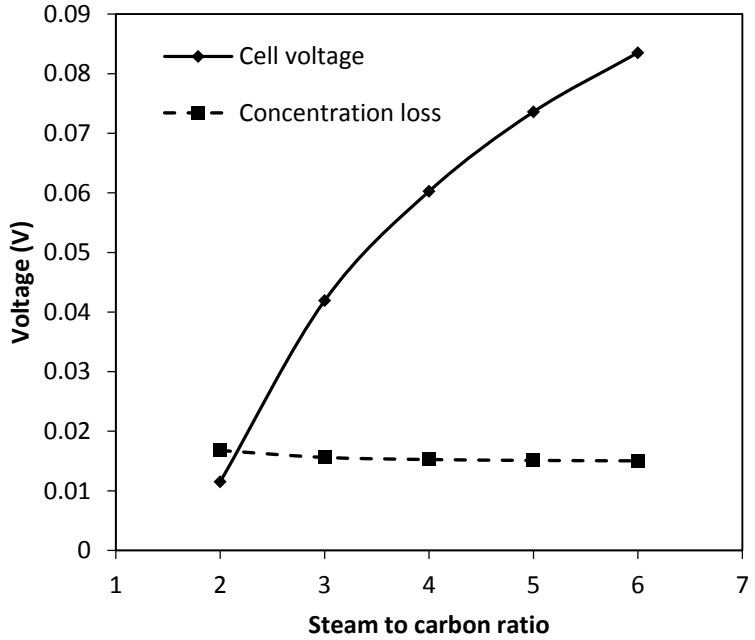

Figure 4.18 Effect of inlet steam to carbon ration at the anode of SOFEC in terms of cell voltage and concentration loss for hydrogen production

4.3.4 Effect of operating pressure

Operating pressure was varied from 1 to 10 bar. As a result, when operating pressure increased, power density consumption decreased at operating pressure from 1 to 3 bar and increased from 3 to 10 bar and efficiency less changed (Figure 4.19). In addition, power consumption decreased at the beginning because the concentration overpotential decreased rapidly at 1-3 bar (Figure 4.20). After that, the concentration overpotential decreased slightly and the OCV of SOFEC continuously increased so power density increased. In addition, the operating pressure do not affect on the activation overpotential and ohmic loss.

4.3.5 Effect of operating temperature

Operating temperature was varied from 873 K to 1273 K. From Figure 4.21, power consumption decreased and efficiency increased with increasing operating temperature. Not only electrochemical reaction but also steam reforming reaction at the anode is faster reaction than reaction before increasing operating temperature. In addition, reduction of electrical energy consumption is occurred when operating temperature increase according to thermodynamics of the SOEC (Section 3.3). Figure 4.22 shows effect of operating temperature on cell voltage and overpotential losses. All of overpotential losses depended on operating temperature. When operating temperature increased, cell voltage, activation overpotential, ohmic loss decreased obviously and concentration overpotential slightly increased because of partial pressure of gases at TPB. Consequently, high operating temperature can improve the performance of the SOFEC however there is a limitation of cell materials.

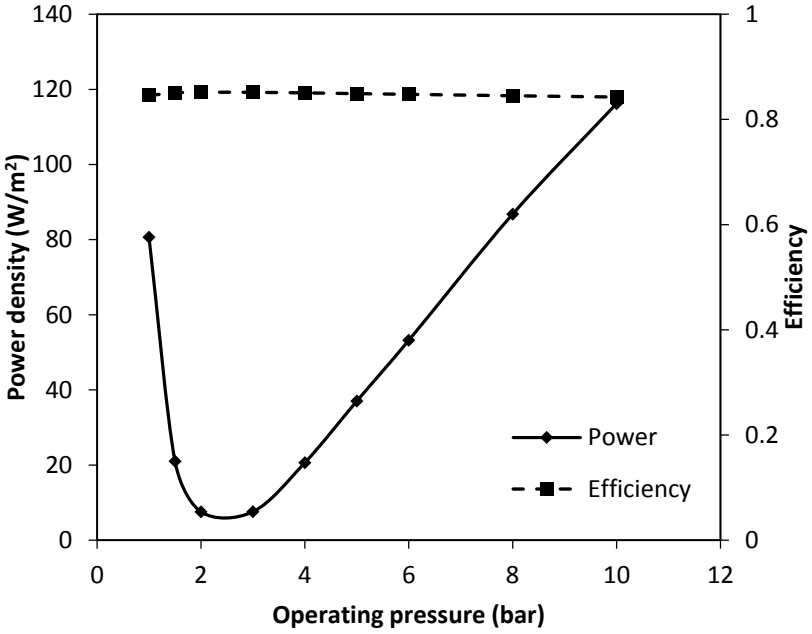

Figure 4.19 Effect of operating pressure of SOFEC on power density and efficiency for hydrogen production

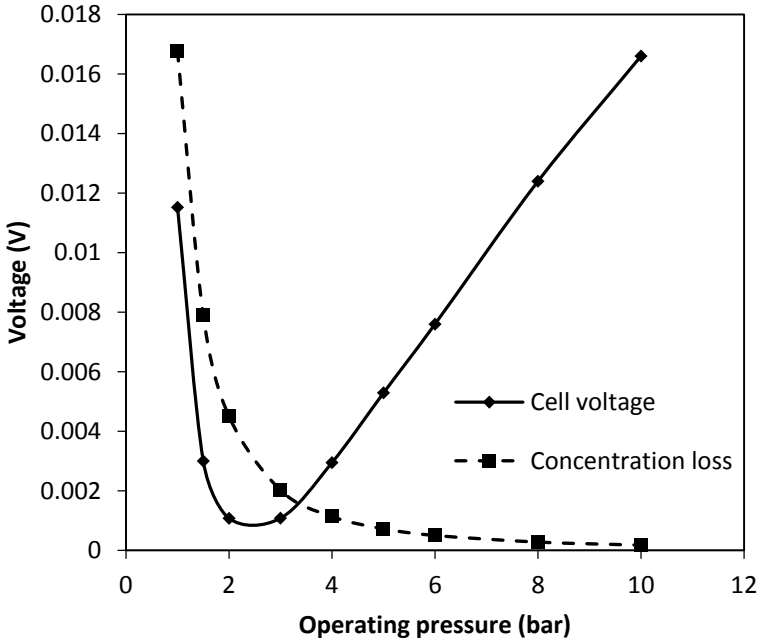

Figure 4.20 Effect of operating pressure of the SOFEC on cell voltage and concentration loss for hydrogen production

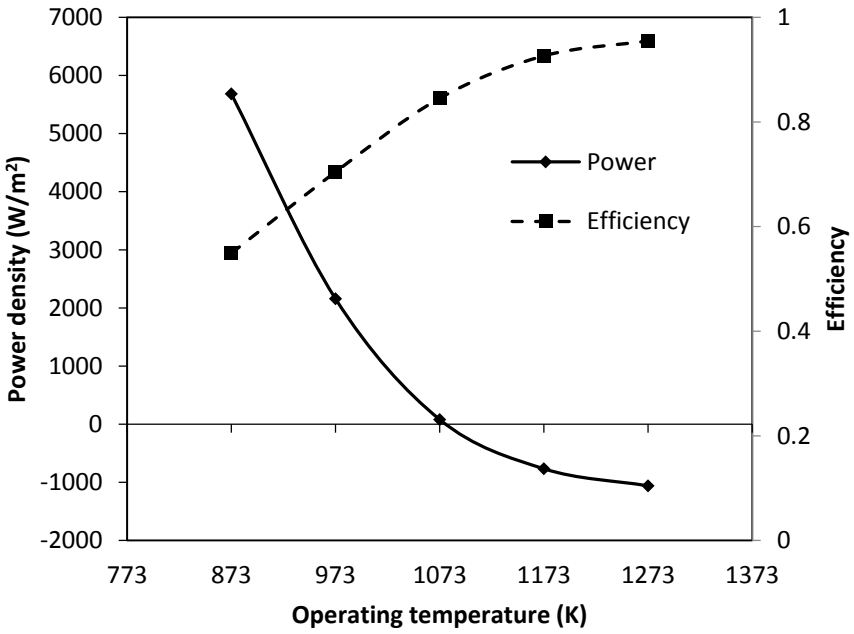

Figure 4.21 Effect of operating temperature of the SOFEC on power density and efficiency for hydrogen production

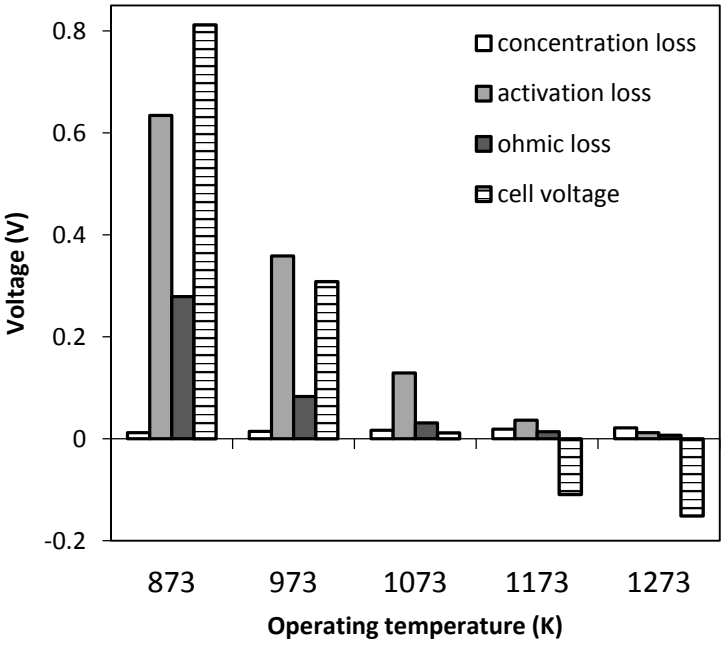

Figure 4.22 Effect of operating temperature of the SOFEC on cell voltage and overpotential losses for hydrogen production

4.3.6 Effect of utilization

4.3.6.1 Effect of steam utilization

Effect of steam utilization at the cathode of SOFEC is presented in Figure 4.23 and Figure 4.24. Steam utilization was varied from 0.5 to 0.9 and fuel utilization was fixed at 0.8. As a result increasing of utilization, power density increase and efficiency less changed (Figure 4.23). Cell voltage and overpotential losses increased with increasing steam utilization in Figure 4.24. In addition, high steam utilization causes high hydrogen production so power consumption increase.

4.3.6.2 Effect of fuel utilization

Effect of fuel utilization at the anode of SOFEC was varied from 0.5 to 0.9 and steam utilization at cathode was fixed at 0.8. Figure 4.25 shows effect of fuel utilization factor on power density and efficiency. Power density and efficiency increased with increasing fuel utilization. Due to increasing fuel utilization, high hydrogen production increased thus cell voltage and overpotential losses increased (Figure 4.26). In addition, fuel utilization is higher effect on the performance of SOFEC than steam utilization because fuel can produce more hydrogen.

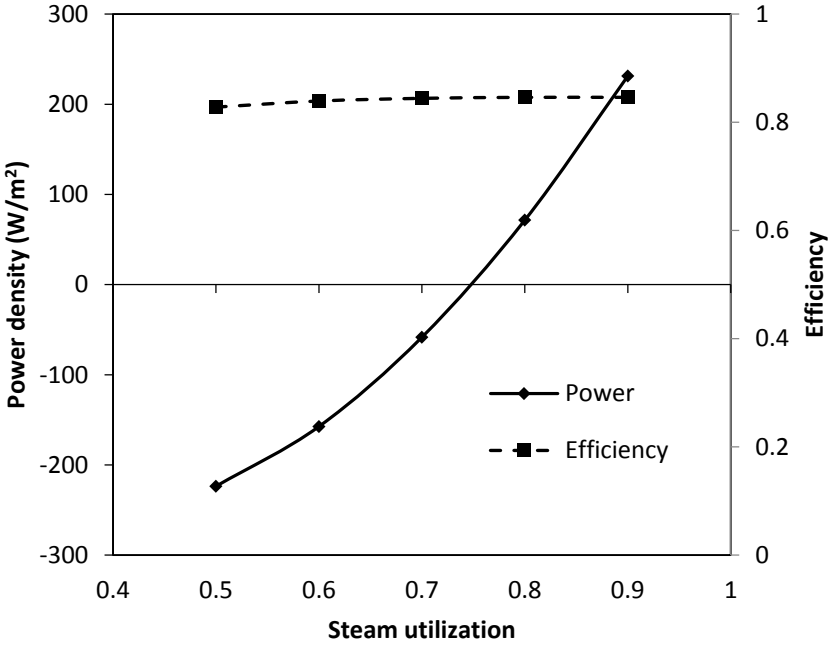

Figure 4.23 Effect of steam utilization at the cathode of SOFEC in terms of power density and efficiency for hydrogen production

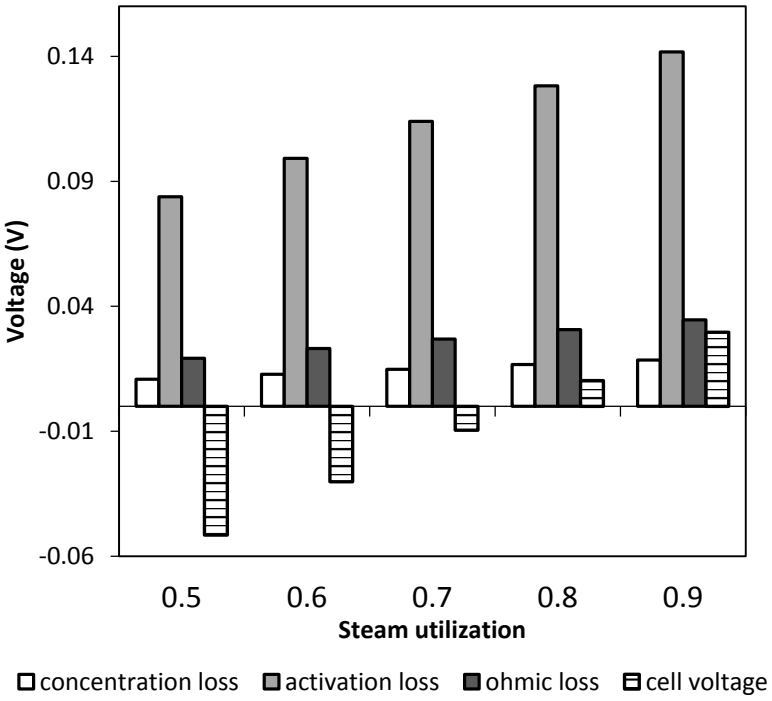

Figure 4.24 Effect of steam utilization at the cathode of SOFEC in terms of cell voltage and overpotential losses for hydrogen production

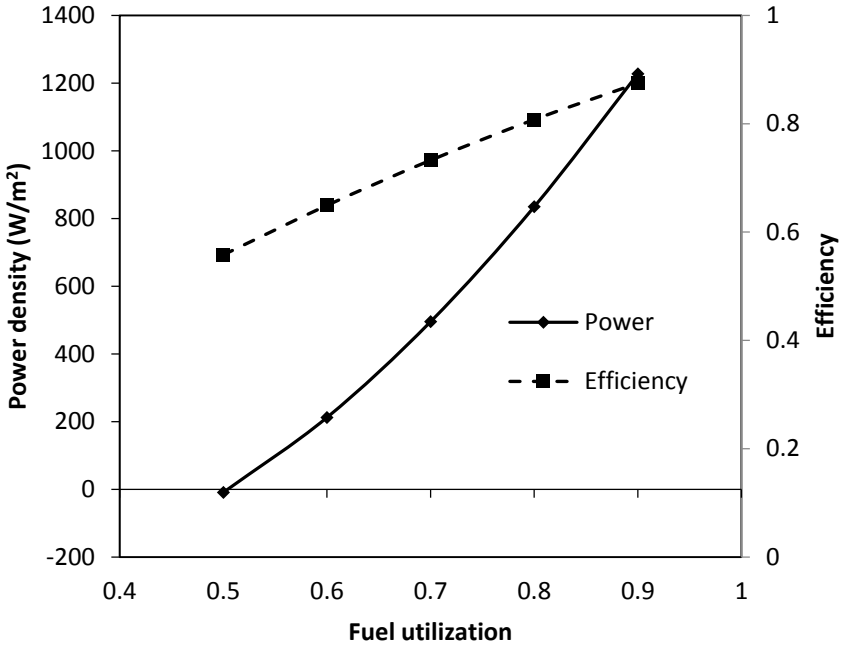

Figure 4.25 Effect of fuel utilization at the anode of SOFEC in terms of power density and efficiency for hydrogen production

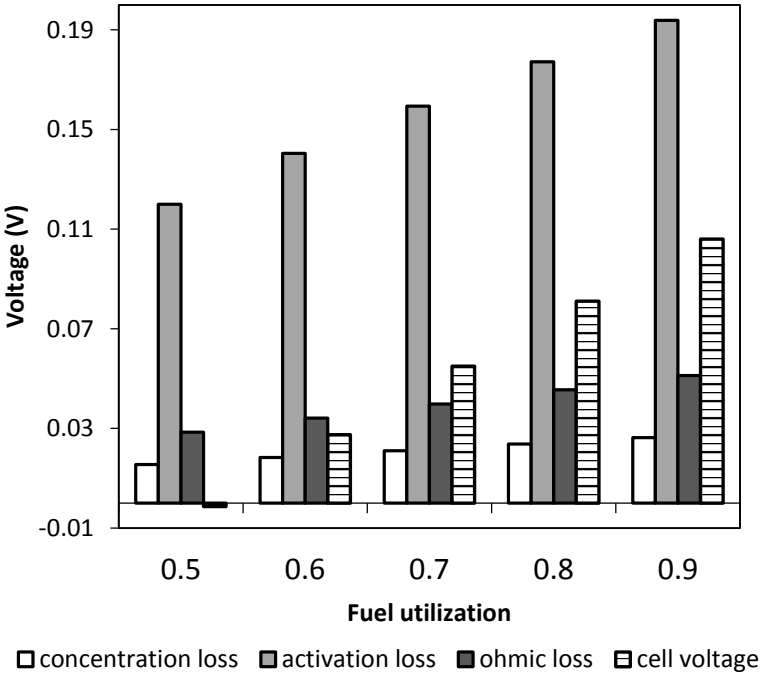

Figure 4.26 Effect of fuel utilization at the anode of SOFEC in terms of cell voltage and overpotential losses for hydrogen production

4.4 Conclusions

The SOFEC for hydrogen production is different from the conventional SOEC by adding methane at the anode side. At the cathode side, steam is fed to the porous cathode and is decomposed into hydrogen and oxygen ion. Next, oxygen ion is transported through the electrolyte to the anode side and reacts with hydrogen from reactions at the anode. At the anode, methane is fed to the anode channel. To avoid carbon deposition, steam is fed to the anode channel too. Thus, the steam reforming and the water-gas shift reaction are occurred. After that, hydrogen from the steam reforming and the water-gas shift reaction reacts with oxygen ion from the electrolyte in order to generate electricity for using in the electrolyzer. The SOFEC is higher performance than the SOEC for hydrogen production in terms of low electrical energy demand. In addition, the SOFEC can run without electrical energy input at zero net cell voltage and can generate electricity at negative cell voltage. The cathode-supported cell is proper to use as the SOFEC for producing hydrogen because of low power demand. Furthermore, electrolyte thickness is significant parameter because it affect on ohmic loss. Thus, electrolyte thickness of 10 μm should be used. High steam fraction at the cathode and high steam to carbon ratio at the anode cause low and high electrical energy consumption, respectively. The steam fraction should be 0.9 and the steam to carbon ratio should be 2. Operating pressure at 2-3 bar are proper for the SOFEC due to low power consumption and operating temperature should be high for using low electrical energy but materials cracking are considered. Moreover, steam utilization and fuel utilization increase, hydrogen production increases, and electrical energy demand increases too.

CHAPTER V

SOLID OXIDE FUEL ASSISTED ELECTROLYSIS CELL FOR SYNGAS PRODUCTION

This chapter presents about the performance of the SOFEC for syngas production. At the cathode, steam and carbon dioxide are fed in to cathode channel and reversible water gas shift reaction and electrochemical reaction are occurred to produce syngas. Next, oxygen ion is transported through the electrolyte to the anode. At the anode, methane and steam are fed into anode channel. Steam reforming and water gas shift reaction are occurred to produce hydrogen. After that, hydrogen react with oxygen ion from the cathode to produce electricity for the electrolyzer for syngas production. The electrochemical model from section 3.4.2.2 is used for investigation. The performance of the SOFEC is analyzed in terms of voltage, power density, and efficiency. In the first step, the SOFEC is compared with the SOEC for syngas production. After that, the configurations of the SOFEC are considered. Furthermore, the key operating parameters such as inlet compositions, operating pressure, operating temperature and utilization are investigated.

5.1 Model input parameters and operating conditions

Table 5.1 and Table 5.2 shows the model input parameters and operating conditions of the SOFEC for syngas production. For the SOEC, the cathode, electrolyte, and anode materials are Ni-YSZ, YSZ, and LSM-YSZ, respectively. However, anode material of the SOFEC is changed to Ni-YSZ for methane oxidation in the anode side.

Table 5.1 Model input parameters of the SOFEC for syngas production

Parameters	Value
Cathode pre-exponential factor, k_{ca}	654×10^{9} $\Omega^{-1}m^{-2}$
Cathode activation energy, E_{ca}	140×10^{3} $J\cdot mol^{-1}$
Cathode electric conductivity, σ_{ca}	80×10^{3} $\Omega^{-1}m^{-1}$
For the SOEC	
Anode pre-exponential factor, k_{an}	235×10^{9} $\Omega^{-1}m^{-2}$
Anode activation energy, E_{an}	137×10^{3} $J\cdot mol^{-1}$
Anode electric conductivity, σ_{an}	8.4×10^{3} $\Omega^{-1}m^{-1}$
For the SOFEC	
Anode pre-exponential factor, k_{an}	654×10^{9} $\Omega^{-1}m^{-2}$
Anode activation energy, E_{an}	140×10^{3} $J\cdot mol^{-1}$
Anode electric conductivity, σ_{an}	80×10^{3} $\Omega^{-1}m^{-1}$
Electrode porosity, ε	0.3
Electrode tortuosity, ξ	6
Average pore radius, r	0.5 μm
Cell length, L	0.4 m
Cell width, W	0.1 m
Cathode thickness, τ_{ca}	50 μm
Electrolyte thickness, τ_{ele}	10 μm
Anode thickness, τ_{an}	500 μm

Parameters (continue)	Value
For comparison of support structures	
For cathode-supported cell	
Cathode thickness, τ_{ca}	500 μm
Electrolyte thickness, τ_{ele}	50 μm
Anode thickness, τ_{an}	50 μm
For electrolyte-supported cell	
Cathode thickness, τ_{ca}	50 μm
Electrolyte thickness, τ_{ele}	500 μm
Anode thickness, τ_{an}	50 μm
For anode-supported cell	
Cathode thickness, τ_{ca}	50 μm
Electrolyte thickness, τ_{ele}	50 μm
Anode thickness, τ_{an}	500 μm

Table 5.2 Operating conditions of the SOFEC for syngas production

Parameters	Value
Operating temperature, T	1073 K
Operating pressure, P	1 bar
Average current density, J	7000 A/m^2
Steam utilization at cathode	0.8
Fuel utilization at anode	0.8
Cathode stream inlet composition	10 mol% H_2, 45 mol% H_2O, 45 mol% CO_2
For the SOEC	
Anode stream inlet composition	100 mol% O_2
For the SOFEC	
Anode stream inlet composition	S/C = 2

5.2 Model validation of the SOEC for syngas production

The simply model of the SOFEC for syngas production is used only electrochemical reaction of steam for co-electrolysis process. To confirm this model can be used for co-electrolysis in the SOEC, the model were compared with experimental data of Ebbesen et al. (2012). The SOEC cell has a 10 – 15 μm thick YSZ electrolyte, a 15–20 μm thick LSM, and a 300 μm thick porous Ni-YSZ layer. The experiments operated at 1023 and 1123 K were compared with the simulation. From Figure 5.1 and Figure 5.2, the comparison of the experimental and model results in terms of polarization curves at different cathode stream inlet composition (25%CO_2-25%H_2O-25%CO-25%Ar and 50%CO_2-25%H_2-25%Ar gas mixtures) and different operating temperature are shown. The model results have also good agreement with the experimental data. Consequently, only electrochemical reduction of steam can be predicted both electrochemical reduction of steam and carbon dioxide. In addition, the simulation results are higher than the experiment because this electrochemical model is not considered the TPB for activation loss.

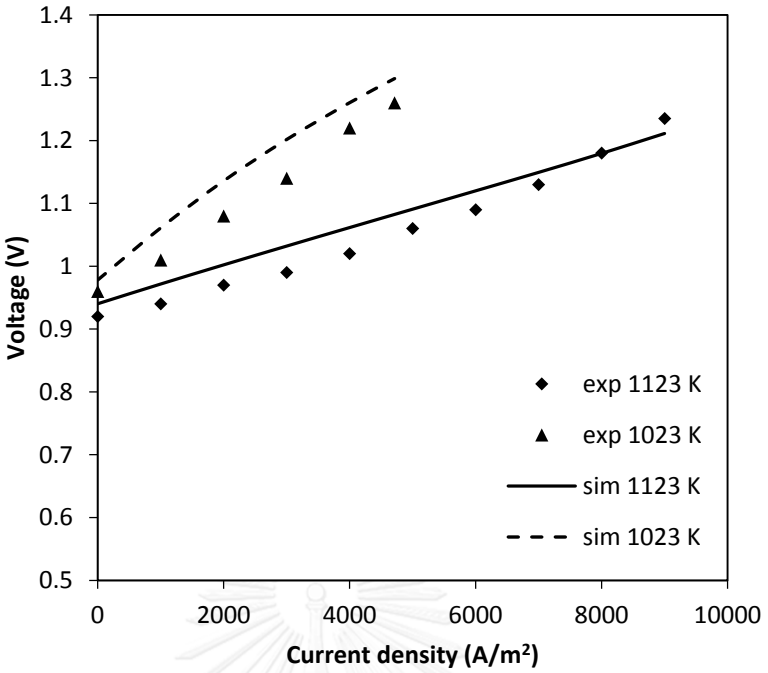

Figure 5.1 Comparison of polarization curves between experimental and model results of the SOFEC at 1023 and 1123 K in 25%CO_2-25%H_2O-25%CO-25%Ar gas mixtures

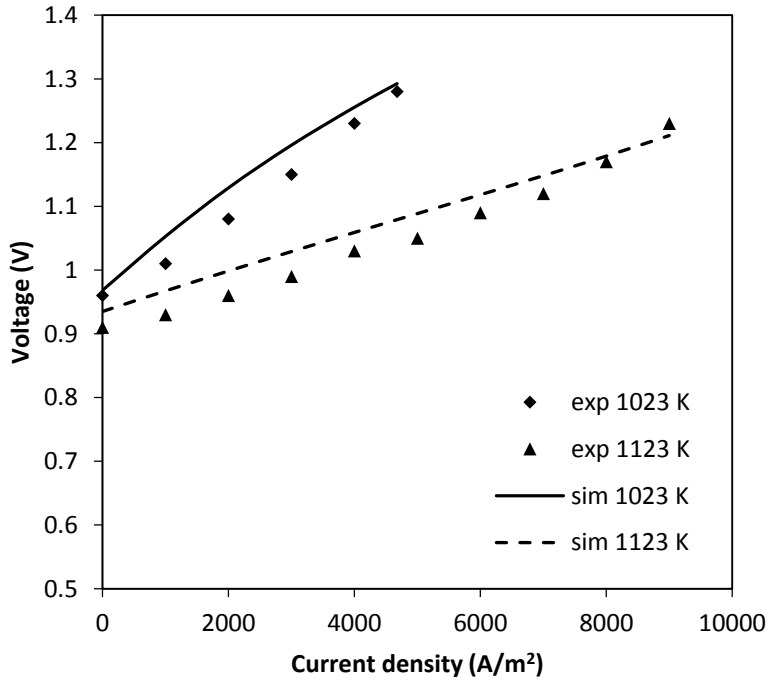

Figure 5.2 Comparison of polarization curves between experimental and model results of the SOFEC at 1023 and 1123 K in 50%CO_2-25%H_2-25%Ar gas mixture

5.3 Results and discussion

5.3.1 Comparisons between the SOEC and the SOFEC for syngas production

The SOEC and the SOFEC for syngas production are different from hydrogen production that carbon dioxide is added to the cathode. In addition, the SOEC and the SOFEC are only different operation at the anode. Figure 5.3 shows the cell voltage and power density comparisons of the SOEC and the SOFEC. As a result, the voltage of the SOFEC is more 1 V lower than the SOEC that is same as the SOFEC for hydrogen production. In addition, current density of the SOFEC at zero voltage for syngas production was lower than hydrogen production because of inlet compositions. Current density from 0 to 6000 A/m^2 has negative voltage, which can generate electricity. The power density of the SOFEC is lower than the SOEC significantly and the maximum power generation is about 215 W/m^2 at current density of 3000 A/m^2. At negative cell voltage, the SOFEC can decrease more than 100% of power demand compared with the SOEC. It means that the SOFEC not only run without electrical energy but also can generate electricity. At positive cell voltage, the SOFEC can decrease more than 90% of electrical energy demand compared with the SOEC. Figure 5.4 shows overpotential losses comparison of the SOEC and the SOFEC. Similar to the SOFEC for hydrogen production, Activation overpotential is major overpotential losses and concentration overpotential is smallest effect on cell voltage. Because of different materials and inlet composition between the SOEC and SOFEC, activation and concentration overpotentials are different from the SOEC. Table 5.3 compares the SOEC and the SOFEC at current density of 7000 A/m^2. Production rate of the SOEC and the SOFEC are same but the SOFEC uses low electrical energy.

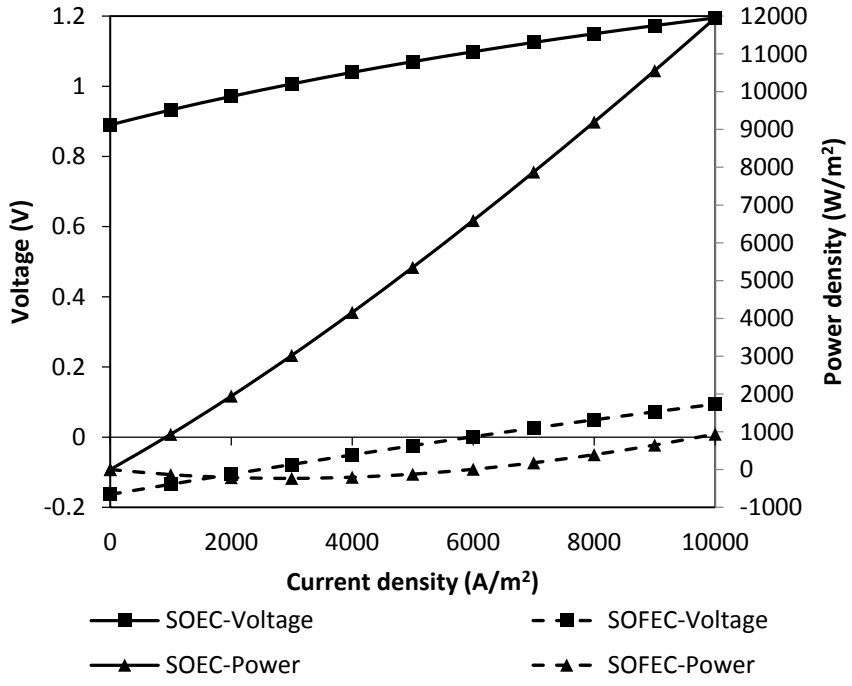

Figure 5.3 Comparison of cell voltage and power density between the SOEC and the SOFEC for syngas production

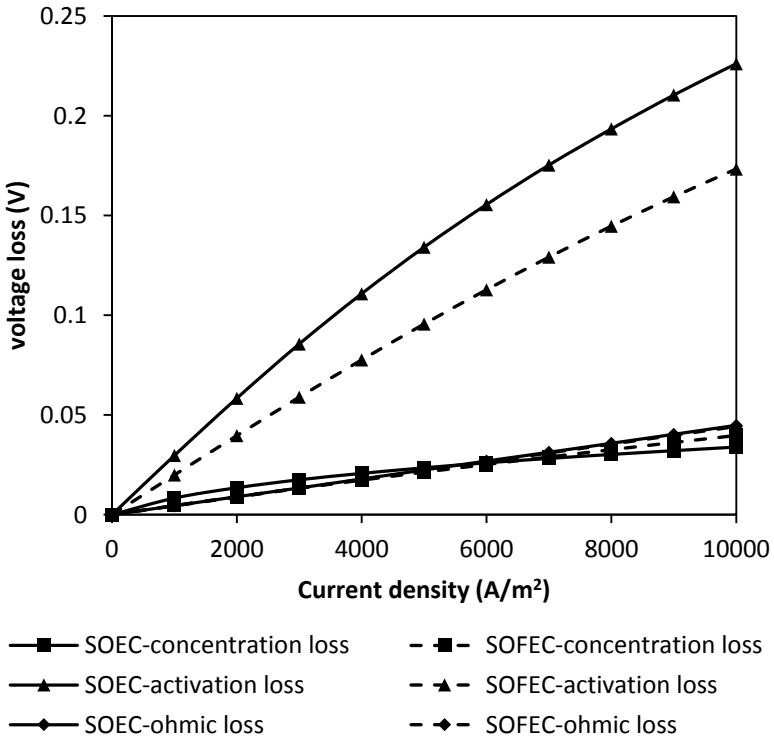

Figure 5.4 Comparison of overpotential losses between the SOEC and the SOFEC for syngas production

Table 5.3 Comparison of the SOEC and the SOFEC for syngas production at current density of 7000 A/m^2

	SOEC	SOFEC
Current density (A/m^2)	7000	7000
Net cell voltage (V)	1.125	0.026
Power density (W/m^2)	7875	179
Concentration overpotential (V)	0.0282	0.0289
Activation overpotential (V)	0.1753	0.1291
Ohmic loss (V)	0.031	0.031
Hydrogen production rate (mol/s)	0.00102	0.00102
Carbon monoxide production rate (mol/s)	0.0008	0.0008
Steam inlet flow rate at cathode (mol/s)	0.00037	0.00037
Methane inlet flow rate at anode (mol/s)	0	0.00045

Figure 5.5 presents flow rate of syngas production, steam and carbon dioxide inlet at the cathode of the SOEC and SOFEC, and methane inlet at anode of the SOFEC at differnt current density. As a result, syngas production rate depends on current density and reversible water gas shift reaction. Hydrogen to carbon monoxide ratio is about 1.28. In addition, hydrogen to carbon monoxide ratio can be designed by adjust inlet composition, current density, pressure, and temperature.

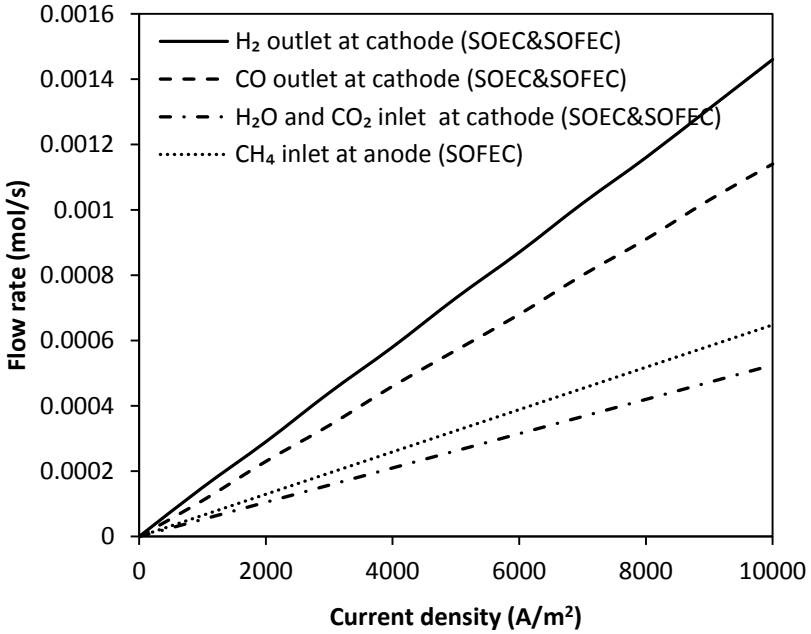

Figure 5.5 Flow rate of hydrogen outlet at the cathode, carbon monoxide outlet at the cathode, steam and carbon dioxide inlet at cathode, and methane inlet at anode at differnt current density of SOEC and SOFEC

5.3.2 Effect of configurations

From Figure 5.6, the cathode-supported, electrolyte-supported, and anode-supported cells were compared in terms of cell voltage. As a result, electrolyte-supported cell had the highest cell voltage while the cathode-supported cell voltage slightly increased from anode-supported cell. Figure 5.7 shows the power density at different configurations. Accordingly to the cell voltage, electrolyte-supported cell had the highest power density while the cell voltage of the cathode-supported slightly increased from anode-supported cell. In addition, electrolyte-supported cell has high voltage because ohmic loss of electrolyte-supported cell is higher than electrode-supported cells obviously (Figure 4.8) thus the electrolyte-supported cell is not suitable for producing syngas via electrolysis process. Besides ohmic loss, concentration loss of each configuration is different too because of the electrode

thickness (Figure 5.8). In Figure 5.8, ‘nconc,ca’ and ‘nconc,an’ represent concentration overpotential at the cathode and anode, respectively. The cathode-supported cell has the highest cathode concentration overpotential. Anode concentration overpotential of the anode-supported cell is second although electrode-supported cells have same thickness electrode because of mole fraction of steam and hydrogen in the electrodes which have an affect on effective diffusivity of the electrode. Therefore, the anode-supported SOFEC is the best supported cell in terms of power demand.

The effect of the electrode and electrolyte thickness on the performance of the SOFEC for syngas production is not considered in this section because it same results with the SOFEC for hydrogen production (Section 4.2.2.2-4.2.2.4).

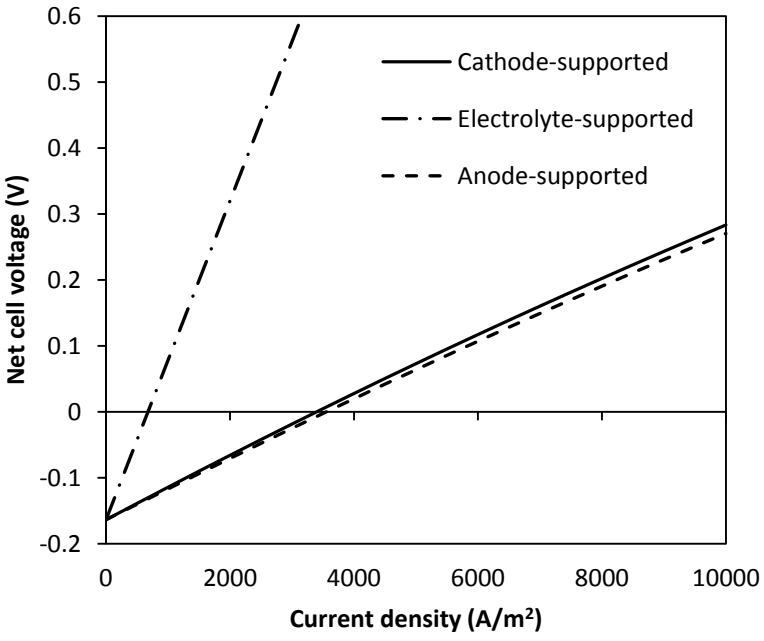

Figure 5.6 Comparison of cell voltage with different supported cell of the SOFEC for syngas production

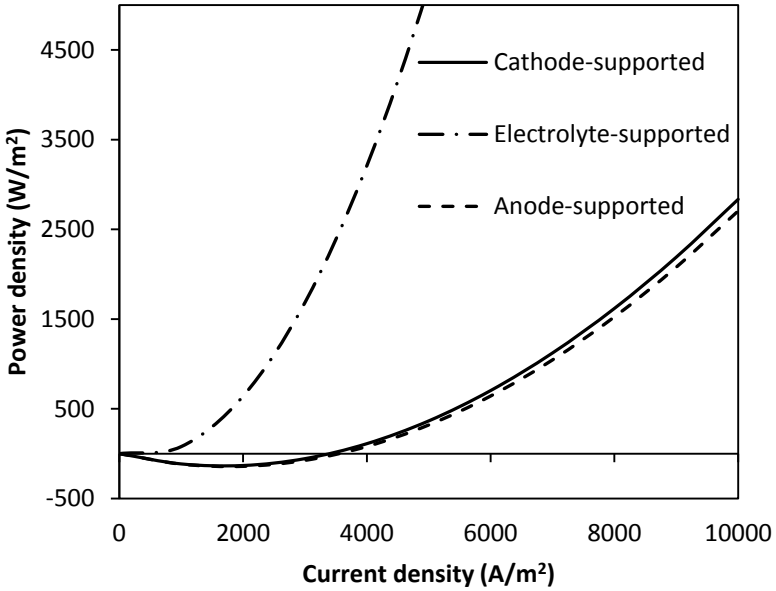

Figure 5.7 Comparison of power density with different supported cell of the SOFEC for syngas production

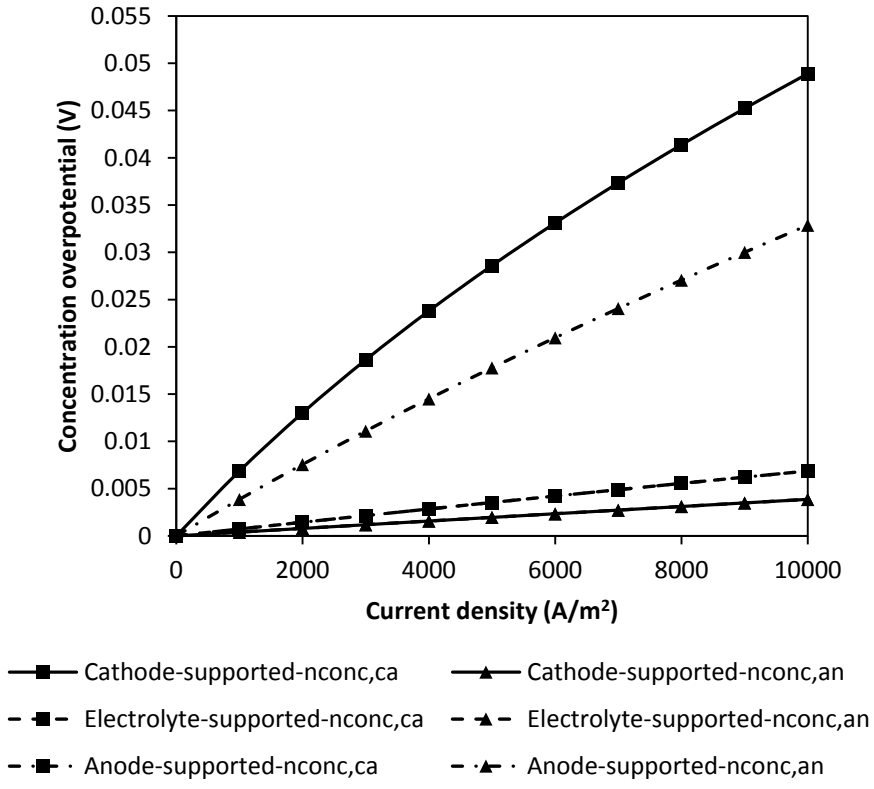

Figure 5.8 Comparison of concentration loss with different supported cell of the SOFEC for syngas production

5.3.3 Effect of inlet composition

For the SOFEC operation for syngas production, steam and carbon dioxide is fed to the cathode. In addition, hydrogen as a reducing gas is added to the cathode too. To study effect of inlet composition, steam molar fraction at the cathode was varied from 15% to 75% with fixed cathode inlet hydrogen fraction at 10% and steam to carbon ratio at the anode at 2. From Figure 5.9, power density demand decreased and efficiency was nearly constant when steam molar fraction increased. The cell voltage decreased in Figure 5.10 because the OCV and concentration overpotential decreased with increasing steam molar fraction.

The effect of inlet steam to carbon ratio on the performance of the SOFEC for syngas production is not considered in this section because it was already analyzed in the SOFEC for hydrogen production (Section 4.2.3.2).

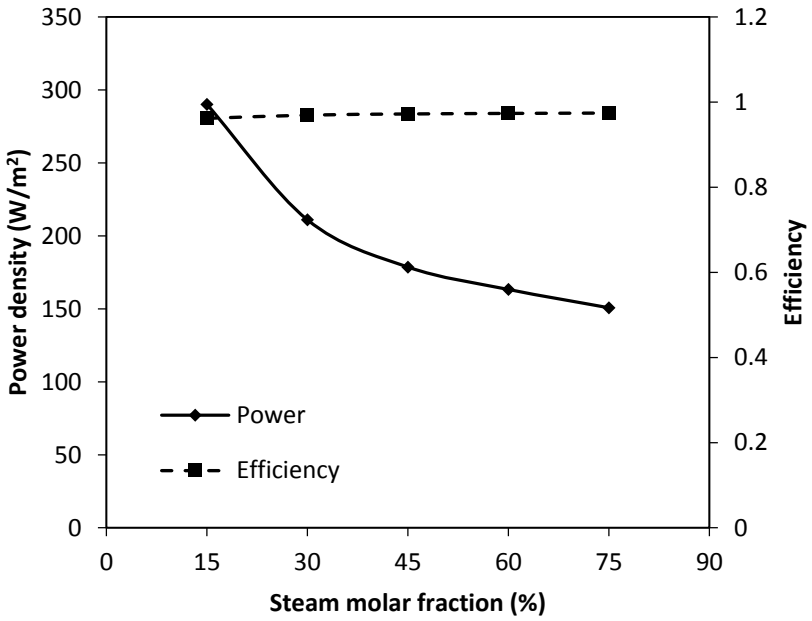

Figure 5.9 Effect of inlet molar fraction at the cathode of SOFEC in terms of power density and efficiency for syngas production

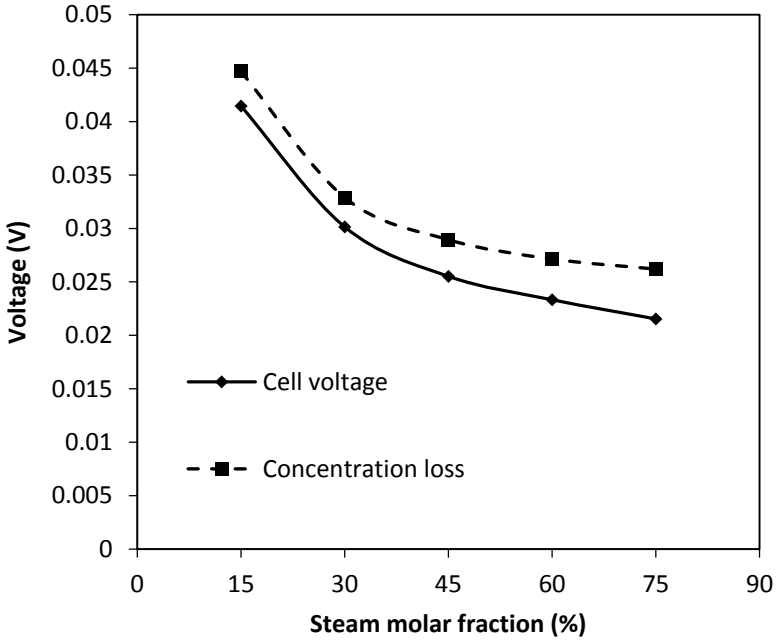

Figure 5.10 Effect of inlet molar fraction at the cathode of SOFEC in terms of cell voltage for syngas production

5.3.4 Effect of operating pressure

Effect of operating pressure on cell voltage, power density, and efficient is investigated. Operating pressure was varied from 1 to 10 bar. As a result, power density decreased from 1 to 3 bar and increased from 3 to 10 bar and efficiency is nearly constant (Figure 5.11). From Figure 5.12, concentration overpotential decreased rapidly from 1 to 3 bar, thus the cell voltage decreased rapidly from 1 to 3 bar. After that, concentration slowly decreased so the cell voltage increased from 3 to 10 bar because the OCV increased with increasing operating pressure.

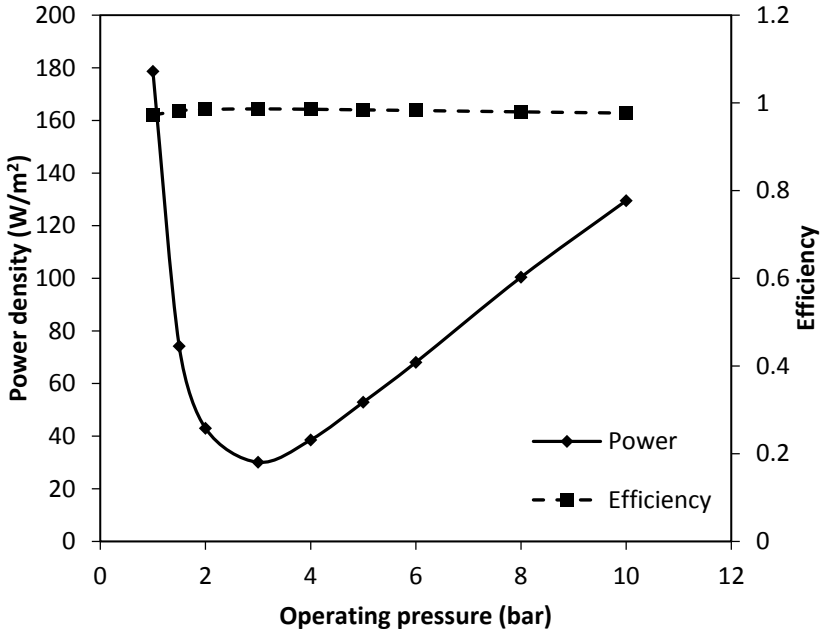

Figure 5.11 Effect of operating pressure of SOFEC on power density and efficiency for syngas production

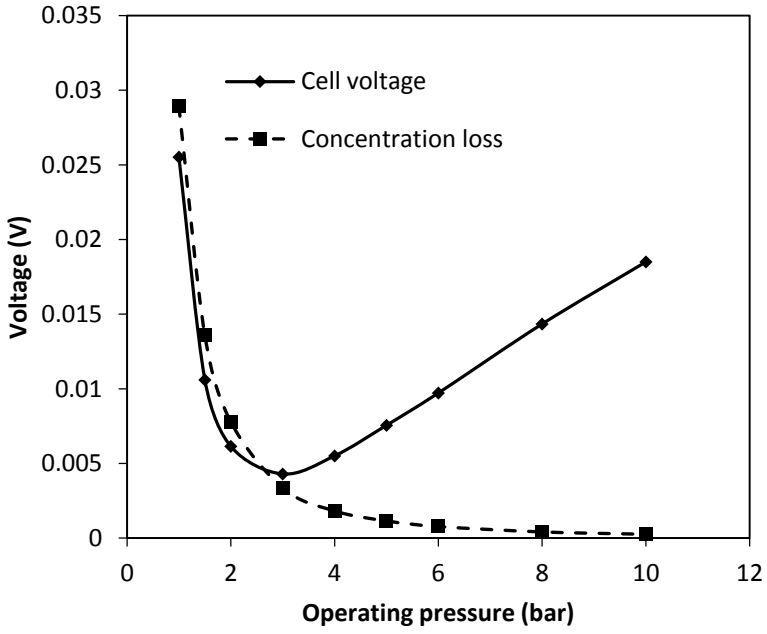

Figure 5.12 Effect of operating pressure of SOFEC on cell voltage and concentration loss for syngas production

5.3.5 Effect of operating temperature

From Figure 5.13, operating temperature was varied from 873 K to 1273 K. It was found that when operating temperature increased, power consumption decreased and efficiency increased. In addition, increasing temperature has an affect on hydrogen production from the steam reforming at anode and reverse water-gas shift at cathode. Furthermore, increasing temperature makes fast reaction and decreased electrical energy demand for electrochemical reaction. Moreover, Activation overpotential is a key overpotential loss that affect on the performance of the SOFEC. From Figure 5.14, it was high activation overpotential when operating temperature decreased. It is noted that, cell voltage and overpotential losses decreased with increasing temperature except concentration overpotential that slowly increased because of partial pressure of gases at TPB.

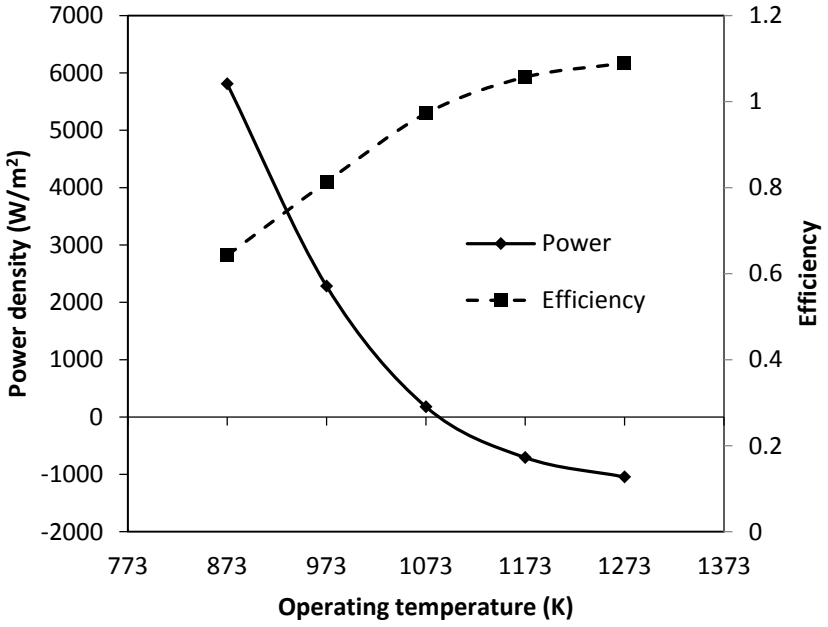

Figure 5.13 Effect of operating temperature of the SOFEC on power density and efficiency for syngas production

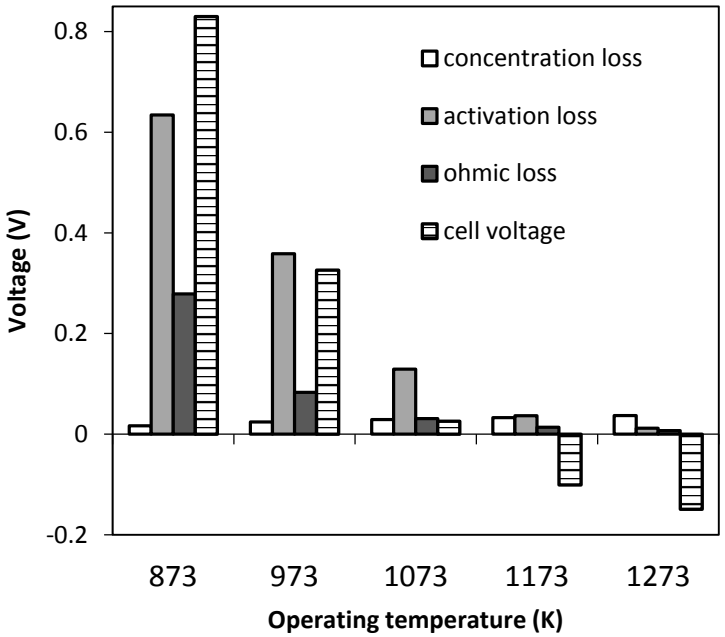

Figure 5.14 Effect of operating temperature of the SOFEC on cell voltage and overpotential losses for syngas production

5.3.6 Effect of utilization

Effect of steam utilization at the cathode of SOFEC for syngas production is analyzed. From Figure 5.15, steam utilization at the cathode was varied from 0.5 to 0.9 and fuel utilization at the anode was fixed at 0.8. When utilization increased, power density increased and efficiency slightly decreased. Power density increased because cell voltage increased with increasing utilization (Figure 5.16). In addition, increasing utilization at the cathode of SOFEC can produce more hydrogen production caused more electrical energy consumption. Activation overpotential is significant overpotential loss that causes cell voltage increase.

The effect of fuel utilization at the SOFEC anode on the performance of the SOFEC for syngas production is not investigated in this section because it was already considered in the SOFEC for hydrogen production (Section 4.2.6.2).

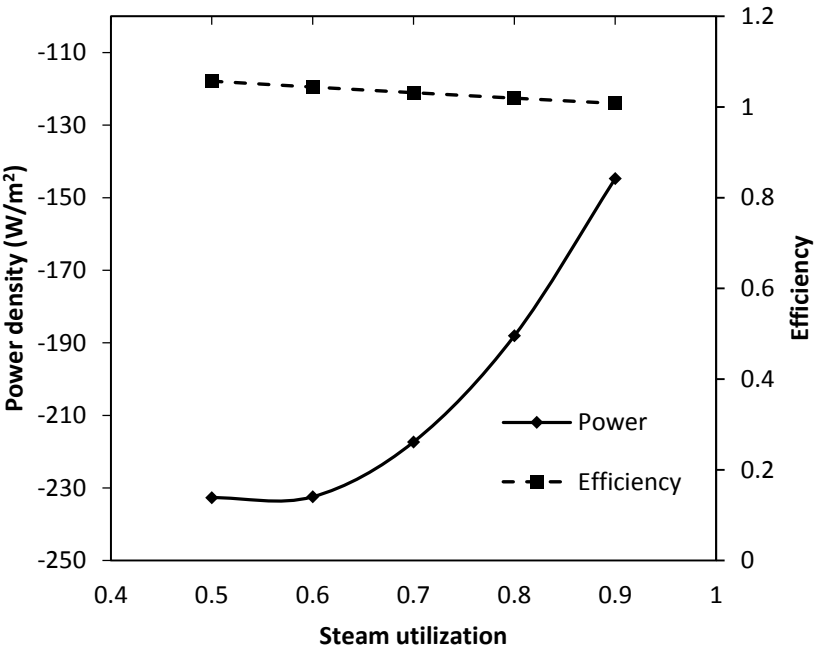

Figure 5.15 Effect of steam utilization at the cathode of SOFEC in terms of power density and efficiency for syngas production

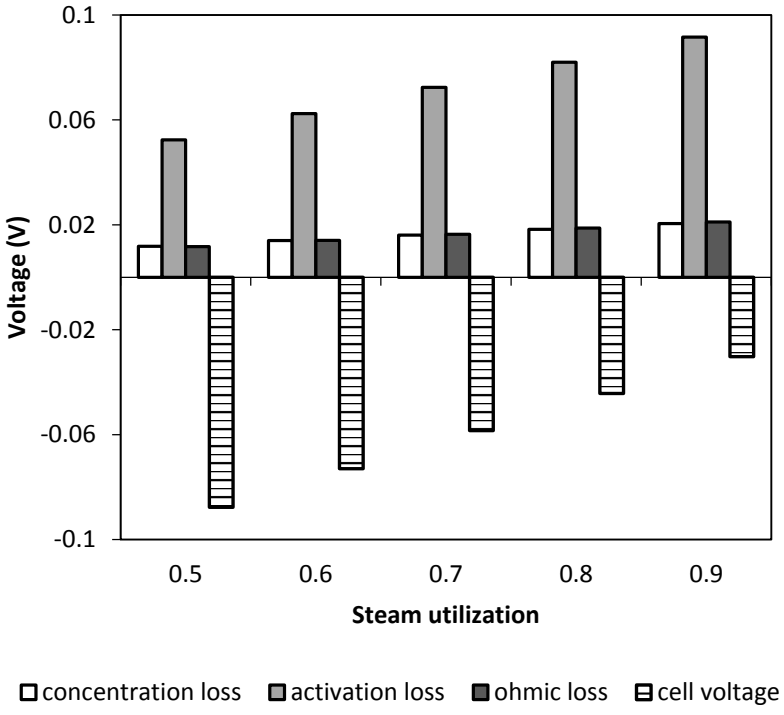

Figure 5.16 Effect of steam utilization at the cathode of SOFEC in terms of cell voltage and overpotential losses for syngas production

5.4 Conclusions

The SOFEC for syngas production is different from the conventional SOEC for syngas production at inlet anode composition. At the cathode, steam and carbon dioxide are fed to the cathode channel. Reversible water gas shift reaction and electrochemical reaction are occurred and production is a syngas. Next, oxygen ion is transported through the electrolyte to the anode side and reacts with hydrogen produced from steam reforming and water gas shift reaction at the anode to produce electricity. At the anode, methane and steam are fed to the anode channel and steam reforming and water gas shift reaction are occurred. The performance of the SOFEC is higher than the SOEC as it requires a lower power input. In addition, the SOFEC can produce both syngas and electricity or can operate without external electrical energy consumption. The anode-supported SOFEC is higher performance than other supported cell due to low power input. High steam fraction at the cathode of the SOFEC causes low electrical energy consumption. Furthermore, operating pressure at 3 bar and high operating temperature are proper for the SOFEC but cell materials cracking is possible if the SOFEC operate at high temperature overmuch. Moreover, when steam utilization increased, power density increased because of increasing syngas production.

CHAPTER VI

CONCLUSIONS AND RECOMMENDATIONS

6.1 Conclusions

A solid oxide fuel-assisted electrolysis cell (SOFEC) is applied from a solid oxide electrolysis cell (SOEC) by adding methane to the anode side. To protect carbon formation at the anode, steam is fed to the anode. Thus, the anode of SOEC behaves like the anode of solid oxide fuel cell (SOFC) that electricity is generated for used in the electrolyzer. In addition, syngas production, which is used as a reactant for synthetic fuel production, can be produced from the SOFEC too. Thus, the SOFEC for hydrogen and syngas production is investigated. A model based on electrochemical model is developed for the SOFEC. As a result for hydrogen and syngas production, the net cell voltage of the SOFEC is about 1 V lower than the SOEC. Electrical energy consumption of the SOFEC decreases more than 100% of the conventional SOEC when negative net cell voltage is occurred and decreases more than 90% of the conventional SOEC when positive net cell voltage is occurred. The SOFEC can produce both hydrogen/syngas and electricity at negative net cell voltage and produce only hydrogen/syngas at positive net cell voltage. The cathode-supported cell is proper to use for hydrogen production and the anode-supported cell is proper to use for syngas production. Furthermore, electrical energy demand increases with increasing steam to carbon ratio at the anode or decreasing steam molar fraction at the cathode of the SOFEC. Operating pressure at about 2-3 bar and high operating temperature have high performance in terms of power input for the SOFEC. However, cell materials cracking is possible if the SOFEC operate at high temperature overmuch. Moreover, when

steam utilization at the cathode and fuel utilization at the anode increase, it causes electrical energy demand increases due to increasing hydrogen and syngas production. In summary, the SOFEC is lower electrical energy consumption, which is mainly hydrogen and syngas production cost, than the SOEC.

6.2 Recommendations

The SOFEC for syngas production should be simulated as a flowsheet of the SOFEC system including heat exchanger, compressor, and steam generator in order to calculate more accurate efficiency. Moreover, the SOFEC system can be designed for high performance such as the SOFEC system with recycle stream.

REFERENCES

Alzate-Restrepo, V., & Hill, J. M. (2008). Effect of anodic polarization on carbon deposition on Ni/YSZ anodes exposed to methane. *Applied Catalysis A: General, 342*(1–2), 49-55. doi: http://dx.doi.org/10.1016/j.apcata.2007.12.039

Becker, W. L., Braun, R. J., Penev, M., & Melaina, M. (2012). Production of Fischer–Tropsch liquid fuels from high temperature solid oxide co-electrolysis units. *Energy, 47*(1), 99-115. doi: http://dx.doi.org/10.1016/j.energy.2012.08.047

Chan, S. H., Khor, K. A., & Xia, Z. T. (2001). A complete polarization model of a solid oxide fuel cell and its sensitivity to the change of cell component thickness. *Journal of Power Sources, 93*(1–2), 130-140. doi: http://dx.doi.org/10.1016/S0378-7753(00)00556-5

De Groot, A. (2003). Methane and hydrogen: on the role of end-use technologies in shaping the infrastructure. In J. H. Reith, R. H. Wijffels & H. Barten (Eds.), *Bio-methane & Bio-hydrogen: status and perspectives of biological methane and hydrogen production* (pp. 29-57). The Netherlands: Smiet Offset: The Hague.

Demin, A., Gorbova, E., & Tsiakaras, P. (2007). High temperature electrolyzer based on solid oxide co-ionic electrolyte: A theoretical model. *Journal of Power Sources, 171*(1), 205-211. doi: http://dx.doi.org/10.1016/j.jpowsour.2007.01.027

Dillig, M., & Karl, J. (2012). Thermal Management of High Temperature Solid Oxide Electrolyser Cell/Fuel Cell Systems. *Energy Procedia, 28*(0), 37-47. doi: http://dx.doi.org/10.1016/j.egypro.2012.08.038

Donitz, W., Edle, E., & Streicher, R. (1990) *Electrochemical hydrogen technologies* (pp. 213). Amsterdam: Elsevier.

Dönitz, W., & Erdle, E. (1985). High-temperature electrolysis of water vapor—status of development and perspectives for application. *International Journal of Hydrogen Energy, 10*(5), 291-295. doi: http://dx.doi.org/10.1016/0360-3199(85)90181-8

Ebbesen, S. D., Knibbe, R., & Mogensen, M. B. (2012). Co-Electrolysis of Steam and Carbon Dioxide in Solid Oxide Cells. *Electrochemical Society. Journal, 159*(8), F482-F489. doi: 10.1149/2.076208jes

Elangovan, S., Hartvigsen, J., Herring, J. S., Lessing, P., O'Brien, J. E., & Stoots, C. (2004, 2-3 October 2003). *Hydrogen Production through High-temperature Electrolysis in a Solid Oxide Cell.* Paper presented at the OECD/NEA, Nuclear Production of Hydrogen: Second Information Exchange Meeting, Argonne, Illinois, USA.

Fouih, Y. E., & Bouallou, C. (2013). Recycling of Carbon Dioxide to Produce Ethanol. *Energy Procedia, 37*(0), 6679-6686. doi: http://dx.doi.org/10.1016/j.egypro.2013.06.600

Haberman, B. A., & Young, J. B. (2004). Three-dimensional simulation of chemically reacting gas flows in the porous support structure of an integrated-planar solid oxide fuel cell. *International Journal of Heat and Mass Transfer, 47*(17–18), 3617-3629. doi: http://dx.doi.org/10.1016/j.ijheatmasstransfer.2004.04.010

Hino, R., Haga, K., Aita, H., & Sekita, K. (2004). 38. R&D on hydrogen production by high-temperature electrolysis of steam. *Nuclear Engineering and Design, 233*(1–3), 363-375. doi: http://dx.doi.org/10.1016/j.nucengdes.2004.08.029

J. E. O'Brien, X. Zhang, R. C. O'Brien, (INL);, G. L. H., J. J. Hartvigsen, E. Elangovan (Ceramatec, I., . . . (NASA—GRC), S. F. (2012). Summary Report on Solid-oxide Electrolysis Cell Testing and Development. Washington, D.C. :: United States. Office of the Assistant Secretary for Nuclear Energy ;.

Jensen, S. H., Larsen, P. H., & Mogensen, M. (2007). Hydrogen and synthetic fuel production from renewable energy sources. *International Journal of Hydrogen Energy, 32*(15), 3253-3257. doi: http://dx.doi.org/10.1016/j.ijhydene.2007.04.042

Kazempoor, P., & Braun, R. J. (2014). Model validation and performance analysis of regenerative solid oxide cells: Electrolytic operation. *International Journal of Hydrogen Energy, 39*(6), 2669-2684. doi: http://dx.doi.org/10.1016/j.ijhydene.2013.12.010

Laguna-Bercero, M. A. (2012). Recent advances in high temperature electrolysis using solid oxide fuel cells: A review. *Journal of Power Sources, 203*(0), 4-16. doi: http://dx.doi.org/10.1016/j.jpowsour.2011.12.019

Li, W., Wang, H., Shi, Y., & Cai, N. (2013). Performance and methane production characteristics of H2O–CO2 co-electrolysis in solid oxide electrolysis cells. *International Journal of Hydrogen Energy, 38*(25), 11104-11109. doi: http://dx.doi.org/10.1016/j.ijhydene.2013.01.008

Luo, Y., Shi, Y., Li, W., Ni, M., & Cai, N. (2014). Elementary reaction modeling and experimental characterization of solid oxide fuel-assisted steam electrolysis cells. *International Journal of Hydrogen Energy, 39*(20), 10359-10373. doi: http://dx.doi.org/10.1016/j.ijhydene.2014.05.018

Martinez-Frias, J., Pham, A.-Q., & M. Aceves, S. (2003). A natural gas-assisted steam electrolyzer for high-efficiency production of hydrogen. *International Journal of Hydrogen Energy, 28*(5), 483-490. doi: http://dx.doi.org/10.1016/S0360-3199(02)00135-0

Matsuzaki, Y., & Yasuda, I. (2000). Electrochemical Oxidation of H_2 and CO in a H_2 - H_2O - CO - CO_2 System at the Interface of a Ni-YSZ Cermet Electrode and YSZ Electrolyte. *Journal of The Electrochemical Society, 147*(5), 1630-1635.

Mingyi, L., Bo, Y., Jingming, X., & Jing, C. (2008). Thermodynamic analysis of the efficiency of high-temperature steam electrolysis system for hydrogen production. *Journal of Power Sources, 177*(2), 493-499. doi: http://dx.doi.org/10.1016/j.jpowsour.2007.11.019

Minh, N. Q., & Takahashi, T. (1995). Chapter 9 - Stack design and fabrication. In N. Q. M. Takahashi (Ed.), *Science and Technology of Ceramic Fuel Cells* (pp. 233-306). Oxford: Elsevier Science Ltd.

Momma, A., Kaga, Y., Takano, K., Nozaki, K., Negishi, A., Kato, K., . . . Akikusa, J. (2005). Experimental investigation of anodic gaseous concentration of a practical seal-less solid oxide fuel cell. *Journal of Power Sources, 145*(2), 169-177. doi: http://dx.doi.org/10.1016/j.jpowsour.2004.12.062

Ni, M. (2010). Modeling of a solid oxide electrolysis cell for carbon dioxide electrolysis. *Chemical Engineering Journal, 164*(1), 246-254. doi: http://dx.doi.org/10.1016/j.cej.2010.08.032

Ni, M. (2012a). 2D thermal modeling of a solid oxide electrolyzer cell (SOEC) for syngas production by H2O/CO2 co-electrolysis. *International Journal of Hydrogen Energy, 37*(8), 6389-6399. doi: http://dx.doi.org/10.1016/j.ijhydene.2012.01.072

Ni, M. (2012b). An electrochemical model for syngas production by co-electrolysis of H2O and CO2. *Journal of Power Sources, 202*(0), 209-216. doi: http://dx.doi.org/10.1016/j.jpowsour.2011.11.080

Ni, M., Leung, M. K. H., & Leung, D. Y. C. (2006). An Electrochemical Model of a Solid Oxide Steam Electrolyzer for Hydrogen Production. *Chemical Engineering & Technology, 29*(5), 636-642. doi: 10.1002/ceat.200500378

Ni, M., Leung, M. K. H., & Leung, D. Y. C. (2006). A modeling study on concentration overpotentials of a reversible solid oxide fuel cell. *Journal of Power Sources, 163*(1), 460-466. doi: http://dx.doi.org/10.1016/j.jpowsour.2006.09.024

Ni, M., Leung, M. K. H., & Leung, D. Y. C. (2007a). Energy and exergy analysis of hydrogen production by solid oxide steam electrolyzer plant. *International Journal of Hydrogen Energy, 32*(18), 4648-4660. doi: http://dx.doi.org/10.1016/j.ijhydene.2007.08.005

Ni, M., Leung, M. K. H., & Leung, D. Y. C. (2007b). Parametric study of solid oxide steam electrolyzer for hydrogen production. *International Journal of Hydrogen Energy, 32*(13), 2305-2313. doi: http://dx.doi.org/10.1016/j.ijhydene.2007.03.001

Ni, M., Leung, M. K. H., & Leung, D. Y. C. (2008). Electrochemical modeling of hydrogen production by proton-conducting solid oxide steam electrolyzer. *International Journal of Hydrogen Energy, 33*(15), 4040-4047. doi: http://dx.doi.org/10.1016/j.ijhydene.2008.05.065

Novosel, B., Avsec, M., & Maček, J. (2008). The interaction of SOFC anode materials with carbon monoxide = Reakcije med anodnimi materiali SOFC in ogljikovim monoksidom. *Materiali in tehnologije, 42*(2), 51-57.

O'Brien, J. E., McKellar, M. G., Stoots, C. M., Herring, J. S., & Hawkes, G. L. (2009). Parametric study of large-scale production of syngas via high-temperature co-electrolysis. *International Journal of Hydrogen Energy, 34*(9), 4216-4226. doi: http://dx.doi.org/10.1016/j.ijhydene.2008.12.021

Pay-Yu, Y., Chin-Hsien, C., Ay, S., & Shih-Hung, C. (2011, 16-18 Sept. 2011). *Simulation study of hydrogen production through solid oxide electrolysis cell.* Paper presented at the Electrical and Control Engineering (ICECE), 2011 International Conference on.

Petipas, F., Brisse, A., & Bouallou, C. (2013). Model-based behaviour of a high temperature electrolyser system operated at various loads. *Journal of Power Sources, 239*(0), 584-595. doi: http://dx.doi.org/10.1016/j.jpowsour.2013.03.027

Pham, A., Wallman, H., & Glass, R. S. (2000). United States Patent No. 6051125.

Quakernaat, J. (1995). Hydrogen in a global long-term perspective. *International Journal of Hydrogen Energy, 20*(6), 485-492.

Redissi, Y., & Bouallou, C. (2013). Valorization of Carbon Dioxide by Co-Electrolysis of CO2/H2O at High Temperature for Syngas Production. *Energy Procedia, 37*(0), 6667-6678. doi: http://dx.doi.org/10.1016/j.egypro.2013.06.599

Smolinka, T., Ojong, E. T., & Garche, J. (2015). Chapter 8 - Hydrogen Production from Renewable Energies—Electrolyzer Technologies. In P. T. M. Garche (Ed.), *Electrochemical Energy Storage for Renewable Sources and Grid Balancing* (pp. 103-128). Amsterdam: Elsevier.

Tao, G., & Virkar, A. (2006). A Reversible Planar Solid Oxide Fuel-Assisted Electrolysis Cell and Solid Oxide Fuel Cell for Hydrogen and Electricity Production Operating on Natural Gas Biogas *Progress Report for the DOE Hydrogen Program* (pp. 24-28).

Todd, B., & Young, J. B. (2002). Thermodynamic and transport properties of gases for use in solid oxide fuel cell modelling. *Journal of Power Sources, 110*(1), 186-200. doi: http://dx.doi.org/10.1016/S0378-7753(02)00277-X

Udagawa, J., Aguiar, P., & Brandon, N. P. (2007). Hydrogen production through steam electrolysis: Model-based steady state performance of a cathode-

supported intermediate temperature solid oxide electrolysis cell. *Journal of Power Sources, 166*(1), 127-136. doi: http://dx.doi.org/10.1016/j.jpowsour.2006.12.081

Udagawa, J., Aguiar, P., & Brandon, N. P. (2008). Hydrogen production through steam electrolysis: Control strategies for a cathode-supported intermediate temperature solid oxide electrolysis cell. *Journal of Power Sources, 180*(1), 354-364. doi: http://dx.doi.org/10.1016/j.jpowsour.2008.01.069

Wanchanthuek, R. (2011). Hydrogen Gas: The Expectation to Be a Promising Sustainable Energy Source. *Burapha Science Journal, 16*, 131-140.

Wang, W., Gorte, R. J., & Vohs, J. M. (2008). Analysis of the performance of the electrodes in a natural gas assisted steam electrolysis cell. *Chemical Engineering Science, 63*(3), 765-769. doi: http://dx.doi.org/10.1016/j.ces.2007.10.026

Wang, W., Vohs, J., & Gorte, R. (2007). Hydrogen Production Via CH4 and CO Assisted Steam Electrolysis. *Topics in Catalysis, 46*(3-4), 380-385. doi: 10.1007/s11244-007-9005-8

Wang, X., Yu, B., Zhang, W., Chen, J., Luo, X., & Stephan, K. (2012). Microstructural modification of the anode/electrolyte interface of SOEC for hydrogen production. *International Journal of Hydrogen Energy, 37*(17), 12833-12838. doi: http://dx.doi.org/10.1016/j.ijhydene.2012.05.093

Yu, B., Zhang, W., Xu, J., Chen, J., Luo, X., & Stephan, K. (2012). Preparation and electrochemical behavior of dense YSZ film for SOEC. *International Journal of Hydrogen Energy, 37*(17), 12074-12080. doi: http://dx.doi.org/10.1016/j.ijhydene.2012.05.063

Zhang, H., Wang, J., Su, S., & Chen, J. (2013). Electrochemical performance characteristics and optimum design strategies of a solid oxide electrolysis cell system for carbon dioxide reduction. *International Journal of Hydrogen Energy, 38*(23), 9609-9618. doi: http://dx.doi.org/10.1016/j.ijhydene.2013.05.155

Zou, Y., Zhou, W., Sunarso, J., Liang, F., & Shao, Z. (2011). Electrophoretic deposition of YSZ thin-film electrolyte for SOFCs utilizing electrostatic-steric stabilized suspensions obtained via high energy ball milling. *International*

Journal of Hydrogen Energy, 36(15), 9195-9204. doi: http://dx.doi.org/10.1016/j.ijhydene.2011.04.187

APPENDIX

VITA

Miss Sirapa Thongdee was born in Bangkok, on July 5, 1990. She received her Bachelor's Degree in Chemical Engineering from Kasetsart University in 2012. After that, she had studied in Chemical Engineering at Chulalongkorn University and joined the Control and System Engineering Research Center.